University of Glasgow
Department of Aerospace Engineering

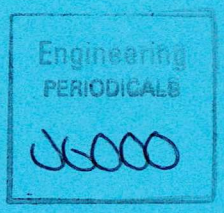

Report On

WIND-TUNNEL TESTS TO DETERMINE THE AERODYNAMIC INDUCED MOMENTS ON THE AZEL AXES OF TWO FORMS OF SENSOR-TURRETS

Prepared
for
GEC-Marconi Avionics Limited

November 27, 1995
Issue 01 Mod 2

Contents

Summary

This report gives the results of the tests carried out to determine the aerodynamic moment loads on the azimuth and elevation axes of two types of sensor-turret model. The two model types are herein referred to as (i) the small-turret and (ii) large-turret. The aerodynamic load was produced by mounting each turret in turn in the flow of the Handley-Page 7 x 5 closed-return wind tunnel, at Glasgow University. A ground board was used to simulate the effect of the interface between the turret assembly and its host.. Each turrets was presented to the flow at orientations

1 Introduction: Instructions for the Tests

Two forms of sensor turret were specified for testing. Both were of the dual orthogonal-axis, Azimuth Elevation (AzEl) arrangement. The instruction for the testing required a controlled steady-state airflow in an environment in which the relevant air-data are measured. The purpose of the test was to estimate the aerodynamic-induced moments on each axis of each turret assemblage under steady-state free stream flow. Further, estimates of the induced moments were required for the range of incident angles of airflow. The specified ranges of airflow incident angles are:

> Azimuth angles from 0 to 360 degrees in steps of 15 Degrees at
> Elevation angles of -90, -45, 0. +45, and +90 degrees.

To carry out the specified tests, two 1:1 scale models were constructed to mimic accurately the configurations of both turrets. The relative orientation of the Azimuth and Elevation axes of both turret models was adjustable through the specified angular ranges. For the tests the models were fitted with calibrated moment (torque) transducers. The tests were performed in the Handley-Page wind tunnel of Department of Aerospace Engineering. Test measurements were automatically logged and retained as a permanent record.

2 Conclusion: The Estimated AzEl Moments.

The data records of the 1000 sample mean torques and their corresponding standard deviation, for each axis of each turret are plotted on the graphs below.

The **small turret's** mean torque records are given in figures 1 through 10, for the azimuth and elevation axis respectively. For comparison figures 41 and 42 are combined graphs of the mean torques for the azimuth and elevation axis respectively.

The **small turret's** standard deviation torque records are given in figures 11 through 20, for the azimuth and elevation axis respectively. For comparison figures 43 and 44 are combined graphs of the mean torques for the azimuth and elevation axis respectively.

The **large turret's** mean torque records are given in figures 21 through 30, for the azimuth and elevation axis respectively. For comparison figures 45 and 46 are combined graphs of the mean torques for the azimuth and elevation axis respectively.

The **large turret's** standard deviation torque records are given in figures 31 through 40, for the azimuth and elevation axis respectively. For comparison figures 47 and 48 are combined graphs of the mean torques for the azimuth and elevation axis respectively.

2.1 Small Turret Mean Torque

fig 1: SMALL TURRET	Azimuth torque at elevation angle of 0 degrees.
fig 2: SMALL TURRET	Elevation torque at elevation angle of 0 degrees.
fig 3: SMALL TURRET	Azimuth torque at elevation angle of -45 degrees.
fig 4: SMALL TURRET	Elevation torque at elevation angle of -45 degrees.
fig 5: SMALL TURRET	Azimuth torque at elevation angle of -90 degrees.
fig 6: SMALL TURRET	Elevation torque at elevation angle of -90 degrees.
fig 7: SMALL TURRET	Azimuth torque at elevation angle of +45 degrees.
fig 8: SMALL TURRET	Elevation torque at elevation angle of +45 degrees.
fig 9: SMALL TURRET	Azimuth torque at elevation angle of +90 degrees.
fig 10: SMALL TURRET	Elevation torque at elevation angle of +90 degrees.

2.2 Small Turret Torque Standard Deviation

fig 11: SMALL TURRET	Azimuth torque standard deviation at elevation angle of 0 degrees.
fig 12: SMALL TURRET	Elevation torque standard deviation at elevation angle of 0 degrees.
fig 13: SMALL TURRET	Azimuth torque standard deviation at elevation angle of -45 degrees.
fig 14: SMALL TURRET	Elevation torque standard deviation at elevation angle of -45 degrees.
fig 15: SMALL TURRET	Azimuth torque standard deviation at elevation angle of -90 degrees.
fig 16: SMALL TURRET	Elevation torque standard deviation at elevation angle of -90 degrees.

fig 17: SMALL TURRET Azimuth torque standard deviation at elevation angle of +45 degrees.

fig 18: SMALL TURRET Elevation torque standard deviation at elevation angle of +45 degrees.

fig 19: SMALL TURRET Azimuth torque standard deviation at elevation angle of +90 degrees.

fig 20: SMALL TURRET Elevation torque standard deviation elevation angle of +90 degrees.

2.3 Large Turret Mean Torque

fig 21: LARGE TURRET Azimuth torque at elevation angle of 0 degrees.

fig 22: LARGE TURRET Elevation torque at elevation angle of 0 degrees.

fig 23: LARGE TURRET Azimuth torque at elevation angle of -45 degrees.

fig 24: LARGE TURRET Elevation torque at elevation angle of -45 degrees.

fig 25: LARGE TURRET Azimuth torque at elevation angle of -90 degrees.

fig 26: LARGE TURRET Elevation torque at elevation angle of -90 degrees.

fig 27: LARGE TURRET Azimuth torque at elevation angle of +45 degrees.

fig 28: LARGE TURRET Elevation torque at elevation angle of +45 degrees.

fig 29: LARGE TURRET Azimuth torque at elevation angle of +90 degrees.

fig 30: LARGE TURRET Elevation torque at elevation angle of +90 degrees.

2.4 Large Turret Standard Deviation

fig 31: LARGE TURRET Azimuth torque standard deviation at elevation angle of 0 degrees.

fig 32: LARGE TURRET Elevation torque standard deviation at elevation angle of 0 degrees.

fig 33: LARGE TURRET Azimuth torque standard deviation at elevation angle of -45 degrees.

fig 34: LARGE TURRET Elevation torque standard deviation at elevation angle of -45 degrees.

fig 35: LARGE TURRET Azimuth torque standard deviation at elevation angle of -90 degrees.

fig 36: LARGE TURRET Elevation torque standard deviation at elevation angle of -90 degrees.

fig 37: LARGE TURRET Azimuth torque standard deviation at elevation angle of +45 degrees.

fig 38: LARGE TURRET Elevation torque standard deviation at elevation angle of +45 degrees.

fig 39: LARGE TURRET Azimuth torque standard deviation at elevation angle of +90 degrees.

fig 40: LARGE TURRET Elevation torque standard deviation elevation angle of +90 degrees.

2.5 Small Turret Combined Data Records

fig 41: SMALL TURRET: Combined azimuth torque data.

fig 42: SMALL TURRET: Combined elevation torque data.

fig 43: SMALL TURRET: Combined azimuth torque standard deviation data.

fig 44: SMALL TURRET: Combined elevation torque standard deviation data.

2.6 Large Turret Combined Data Records

fig 45: LARGE TURRET: Combined azimuth torque data.

fig 46: LARGE TURRET: Combined elevation torque data.

fig 47: LARGE TURRET: Combined azimuth torque standard deviation data.

fig 48: LARGE TURRET: Combined elevation torque standard deviation data.

3 Details of the Sensor-Turret Models

The turret models were manufactured with Medium Density Fibre Board (MDFB). This material high stability and good precision-machining properties. The manufacturing tolerance for both turret models was within 0.0254 mm.

The elevation assemblage was attached to the azimuth axis through a trust bearing. A torque cell to measure the azimuth moment passed though the centre of the thrust bearing an attached to the elevation axis support frame. The other end of the torque cell was secured to the mechanical ground body of the wind tunnel. Elevation axis of the inner gimbals' assemblage was supported at one end by a ball bearing and at the other end by the elevation moment torque cell.

To allow the measurement of aerodynamically induced moments over the specified range of incident angles, provision was made to fix the elevation axis at a specified orientation angle and adjust the azimuth orientation angle with the tunnel flow on. Adjustment of the elevation axis angle required the tunnel flow off.

The arrangement for mounting the turret models in the wind tunnel and method of attaching the moment measuring transducer was the same for both turrets. The azimuth axis assemblage was secured to the mechanical ground of the tunnel which in this particular case is the ground board. The orientation of the turrets in the tunnel

was such as to make the azimuth assemblage the base on which the elevation assemblage was supported.

4. Details of the Wind-Tunnel

The wind tunnel used for the tests is the Department of Aerospace Engineering's Handley-Page wind tunnel. This tunnel is situated in the University of Glasgow Engineering Annex at Spencer street. The tunnel has a octagonal working section with central axis dimension of 7 feet (2.1336 metres) width and 5 feet (1.524 metres) height. The tunnel constant, defined as

$$\frac{\text{Settling Chamber Pressure} - \text{Working Section Wall Pressure}}{\text{Dynamic Pressure}} = 1.14$$

A ground board was installed in the tunnel's working section, below the axis of the free-stream flow. The purpose of this apparatus was to create a boundary layer effect where the turret assemblages attach to their host vehicle and allow the alignment of the turret axes intersection with the centre of the tunnel's working section.

5. Details of the Moment Measuring and Data Acquisition System

The aerodynamically induced moments on both the Azimuth and Elevation axes were measured by identical torque cells. The torque cells were supplied by Aerotech Ltd as factory calibrated units, serial numbers 0272 and 0273. A matched signal conditioning unit mapped the raw torque-cell data from a 4 active-arm sensor bridge to an output voltage. This out voltage was calibrated and scaled according to the following table 2.

Table 2: Torque Cell Data

TORQUE CELL SERIAL No	TRANSFER COEFFICIENT Nm/Volt	ERROR % FSD
0272	5.999	0.06%
0273	5.998	0.06%

The torque cells were designed for a maximum load range of ±30Nm which in turn corresponds to a signal conditioned output of ±5 volts. The signal conditioned outputs were also filtered by a second order low-pass filter with a 100Hz -3dB cut-off.

The data acquisition system was a PC based apparatus. The PC was fitted with the National Instruments DAQ PC-LPM-16. Two channels of 8 differential channel unit sampled the analogue data from the torque cells at the rate of 100 samples per second. The DAQ converted the ±5 volt full-scale samples' amplitudes into 12 bit offset binary code.

The recorded data was scaled to give a direct estimate of the axis torques. The scaling constant was determined by applying a known torque to the each axis of each turret.

6 Data Reduction Methodology

The 12 bit offset binary data samples were collected over a 10 second cycle. The mean and standard deviation for each cycle was computed to establish the aerodynamically induced-moment data point. Therefore each data point is based on the statistics of 1000 samples and so approximates normal distribution statistics. The mean moment and the corresponding standard deviation for the ten seconds record of each data point were computed respectively according to the equations:

$$\overline{X} = \frac{\sum_{i=1}^{1000} x_i}{1000}$$

$$\sigma = \sqrt{\frac{\sum_{i=1}^{1000} (x_i - \overline{X})^2}{1000}}$$

7 Test Results and Estimated Moments

The free-stream flow speed of 50 metres per second was reasonably assumed to test both turret models in their turbulent flow regime. Therefore at higher subsonic airspeeds the aerodynamic behaviour would be observed in the same Reynolds number zone. Under these conditions the relationship between the measured estimate of moment and the calculated estimate of moment is proportional the square of the free-stream air speed.

DEFINITION OF GEOMETRY USED IN THE TEST RECORDS

SIDE VIEW

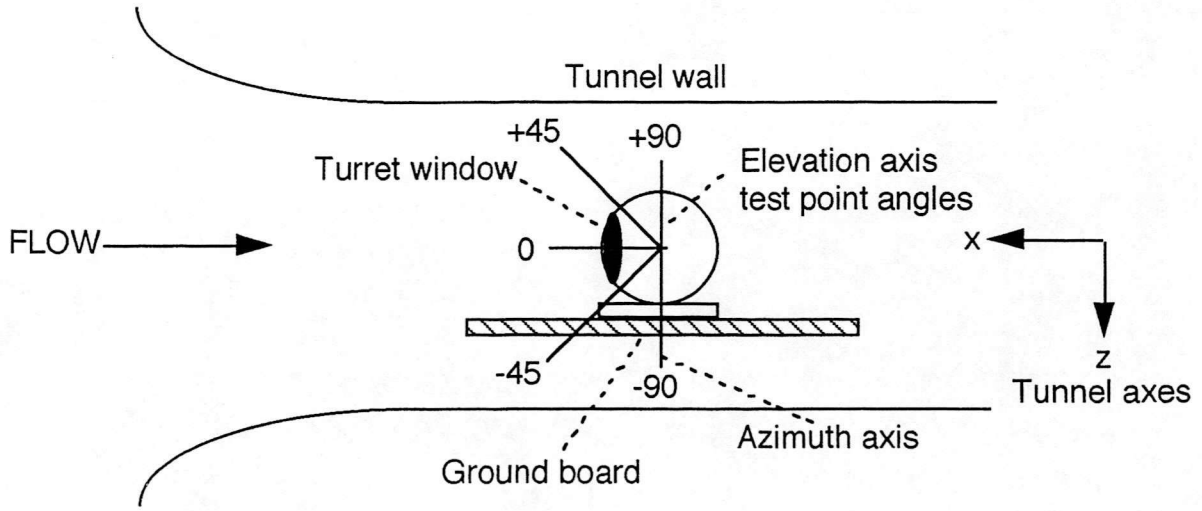

PLAN VIEW

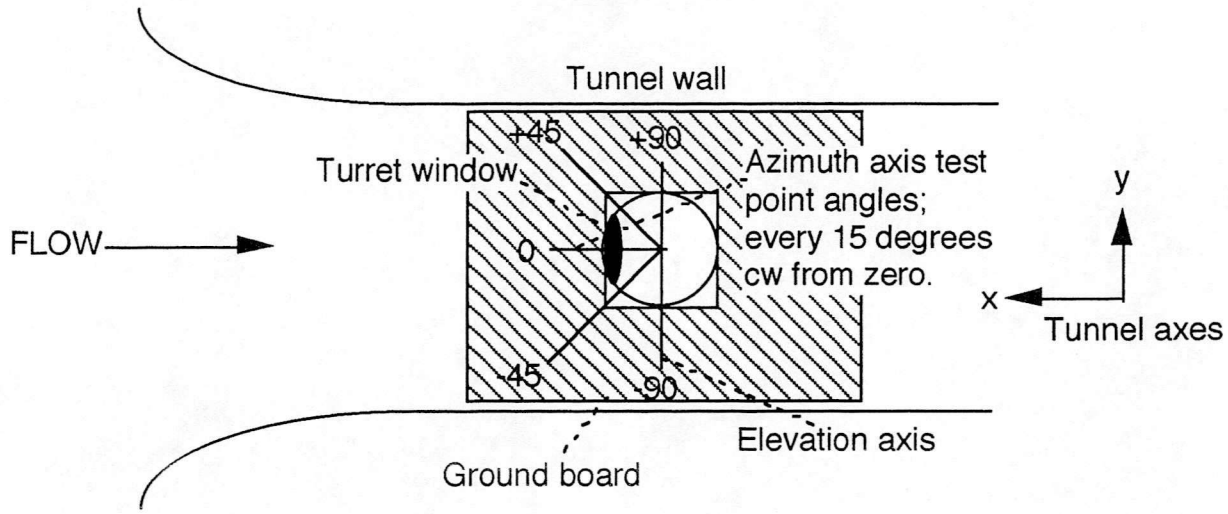

fig 1. SMALL TURRET: Azimuth torque at elevation angle of 0 degrees

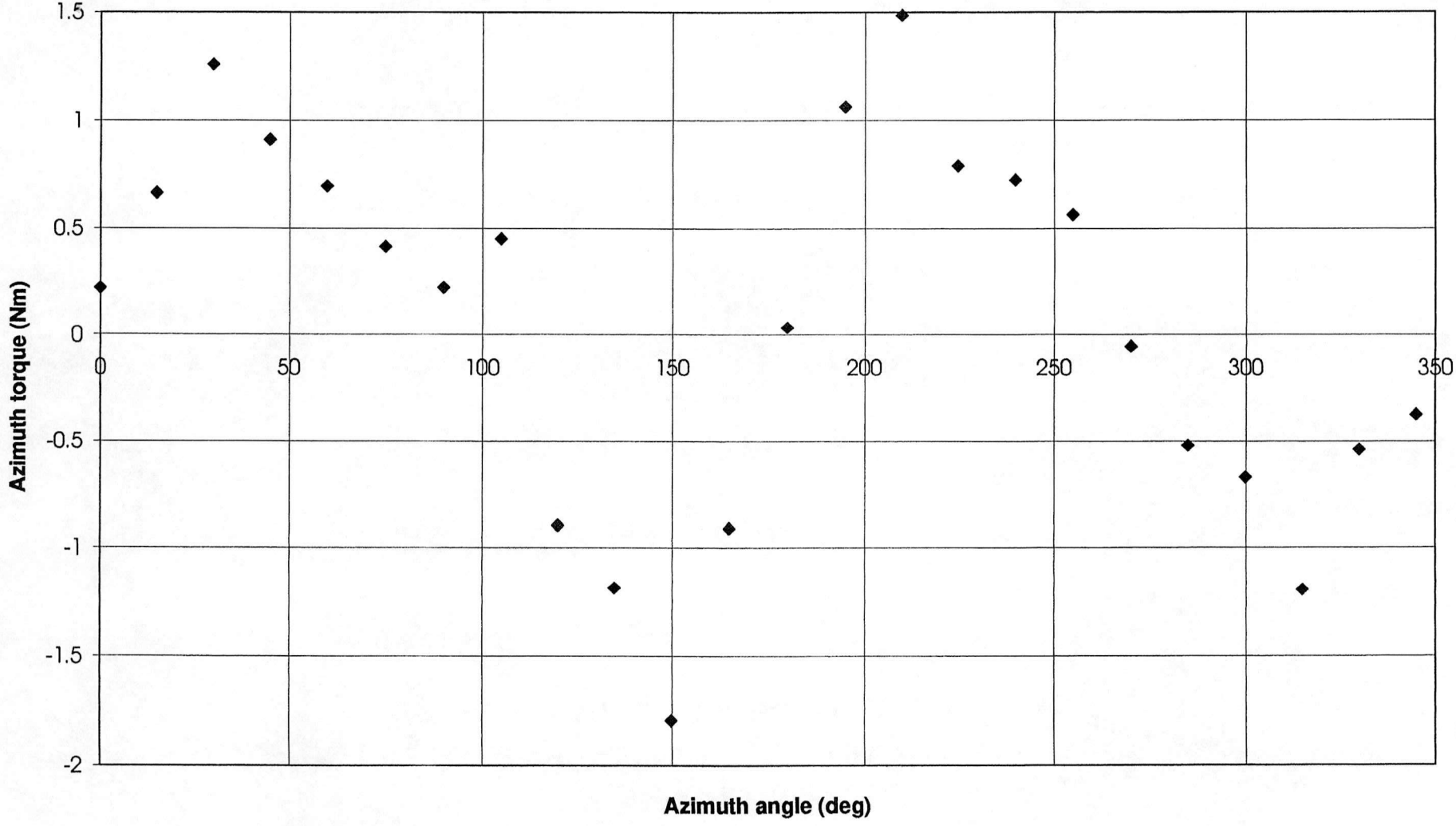

fig 2. SMALL TURRET: Elevation torque at an elevation angle of 0 degrees

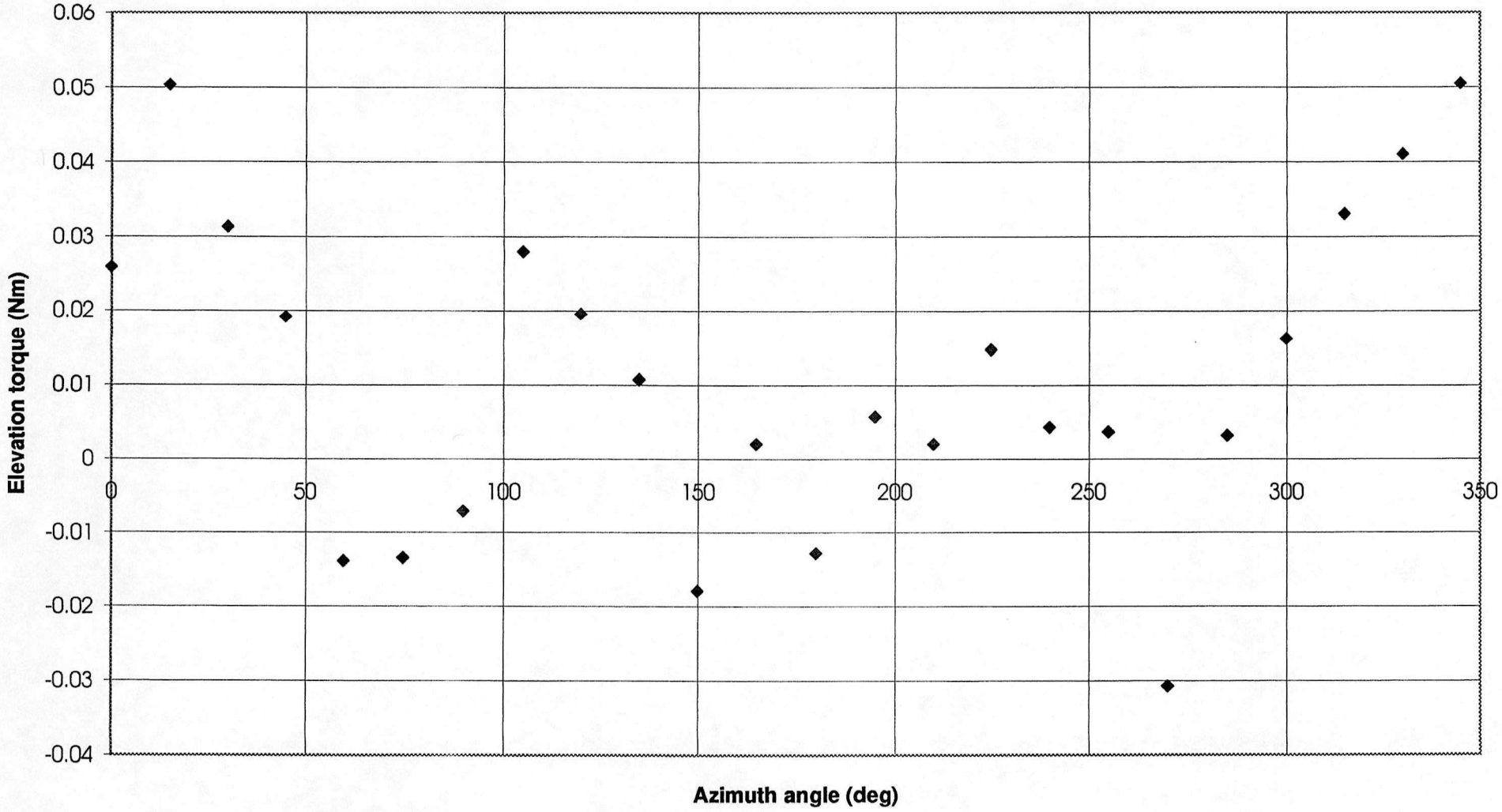

fig 3. SMALL TURRET: Azimuth torque at elevation angle of -45 degrees

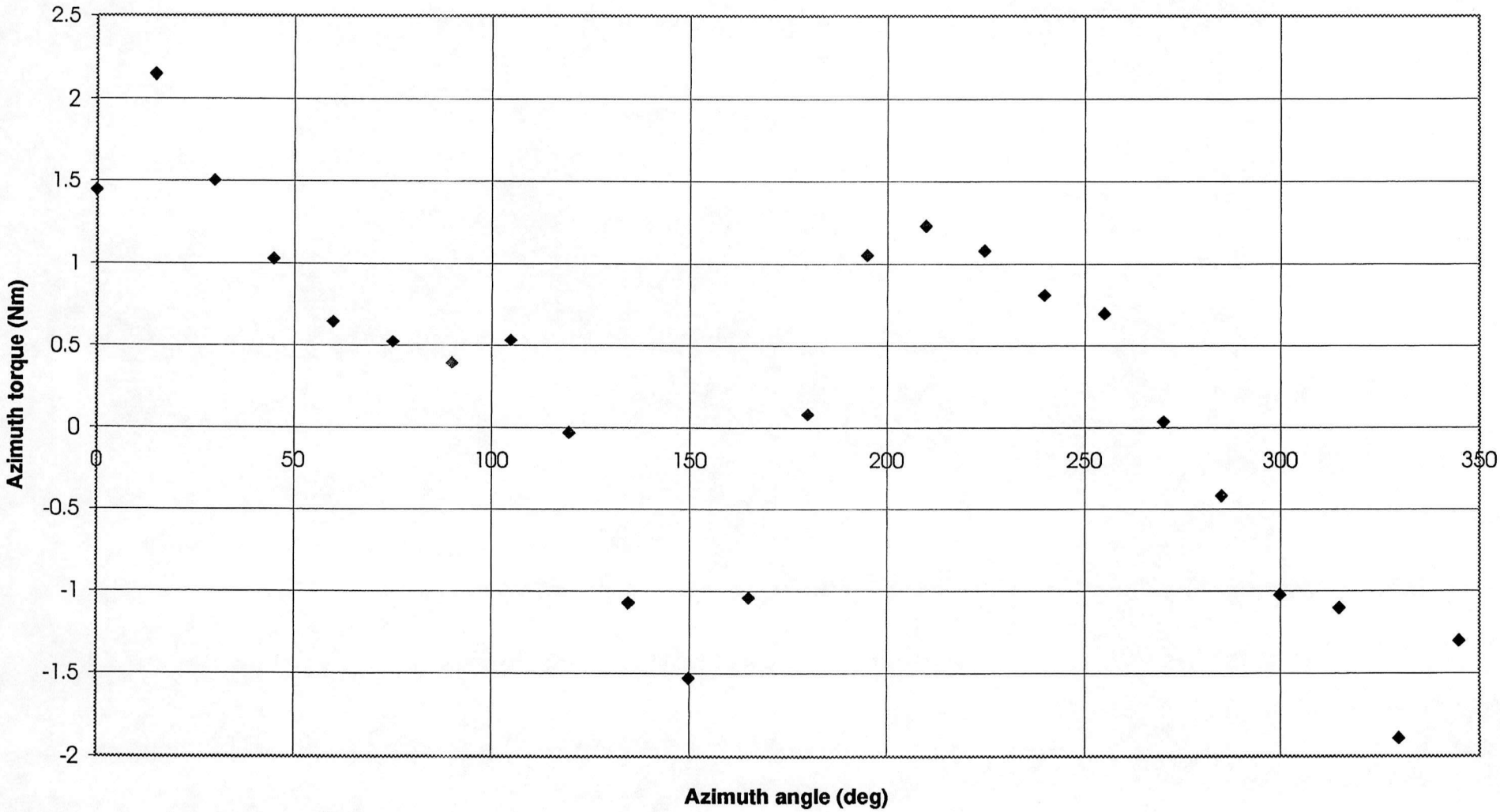

fig 4. SMALL TURRET: Elevation torque at elevation angle of -45 degrees

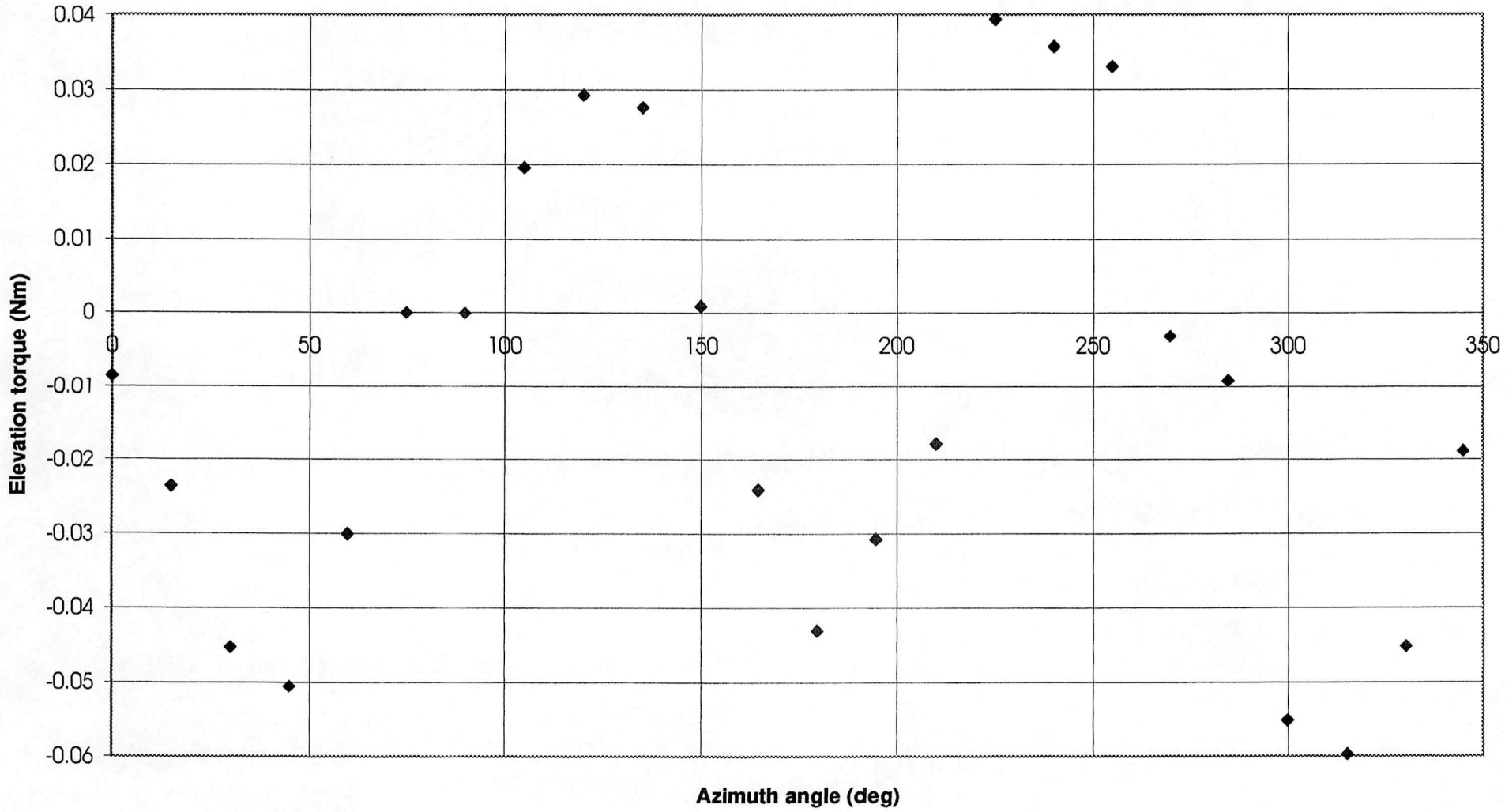

fig 5. SMALL TURRET: Azimuth torque at elevation angle of -90 degrees

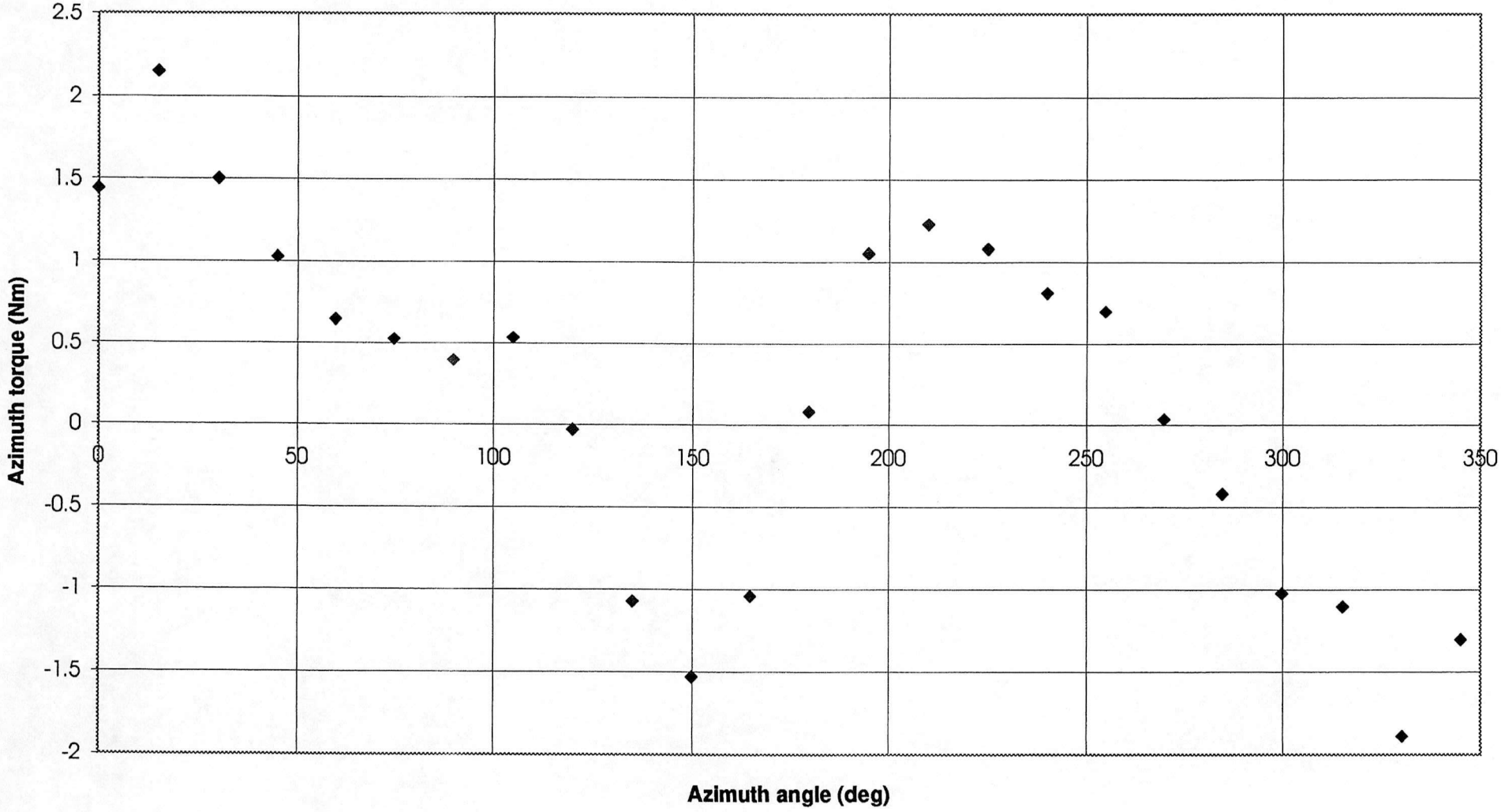

fig 6. SMALL TURRET: Elevation torque at elevation angle of -90 degrees

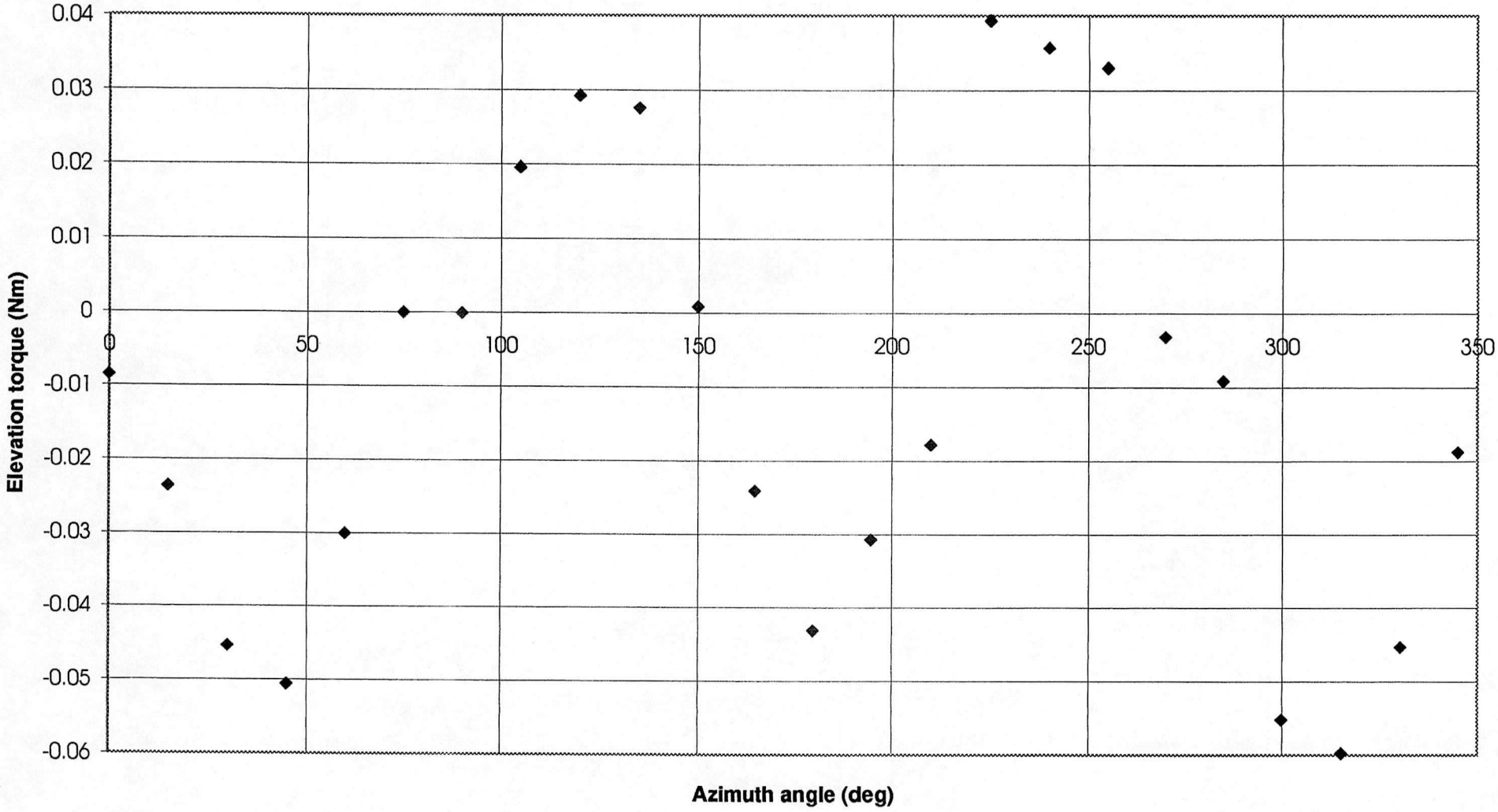

fig 7. SMALL TURRET: Azimuth torque at elevation angle of 45 degrees

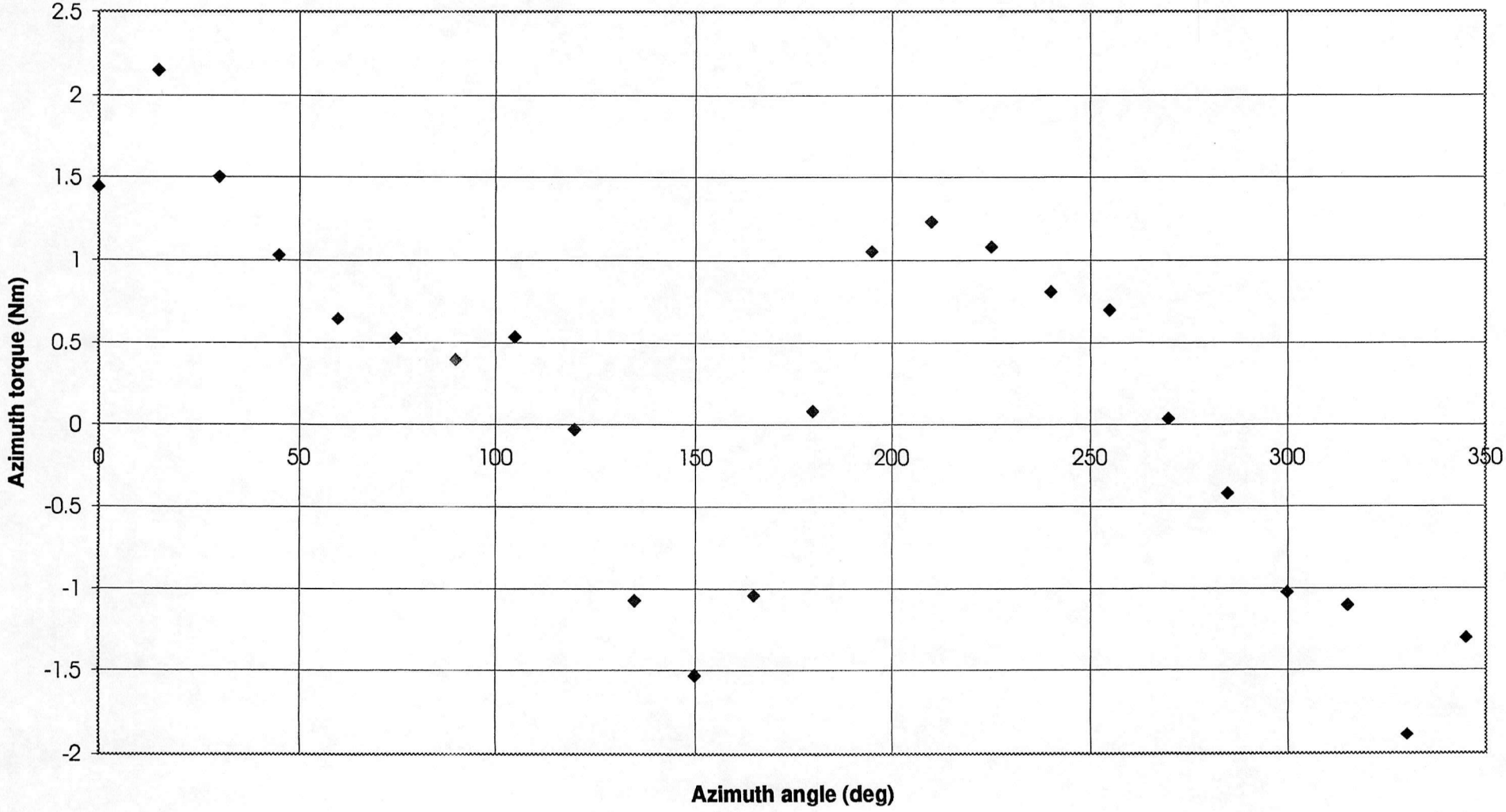

fig 8. SMALL TURRET: Elevation torque at elevation angle of 45 degrees

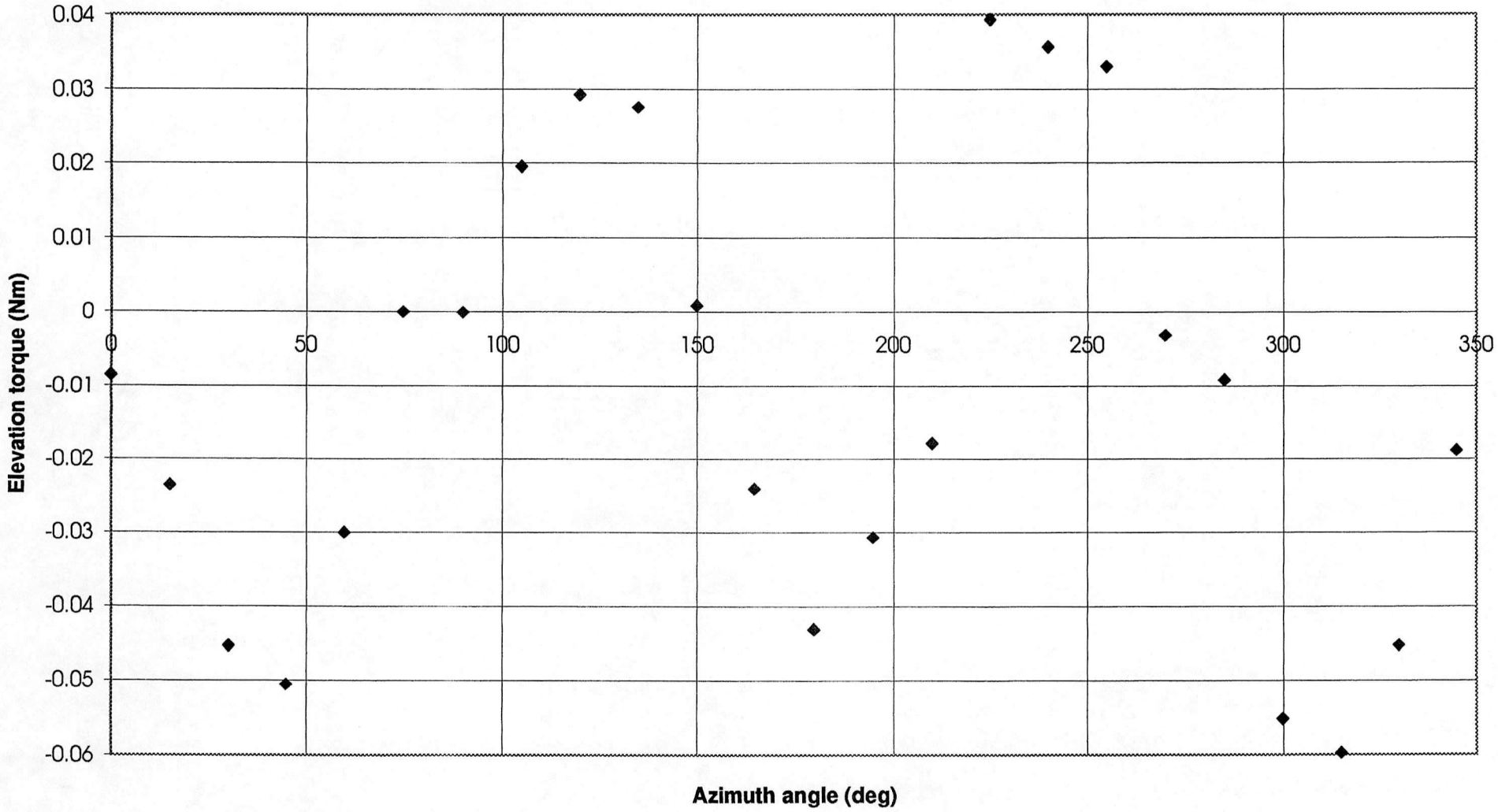

fig 9. SMALL TURRET: Azimuth torque at elevation angle of 90 degrees

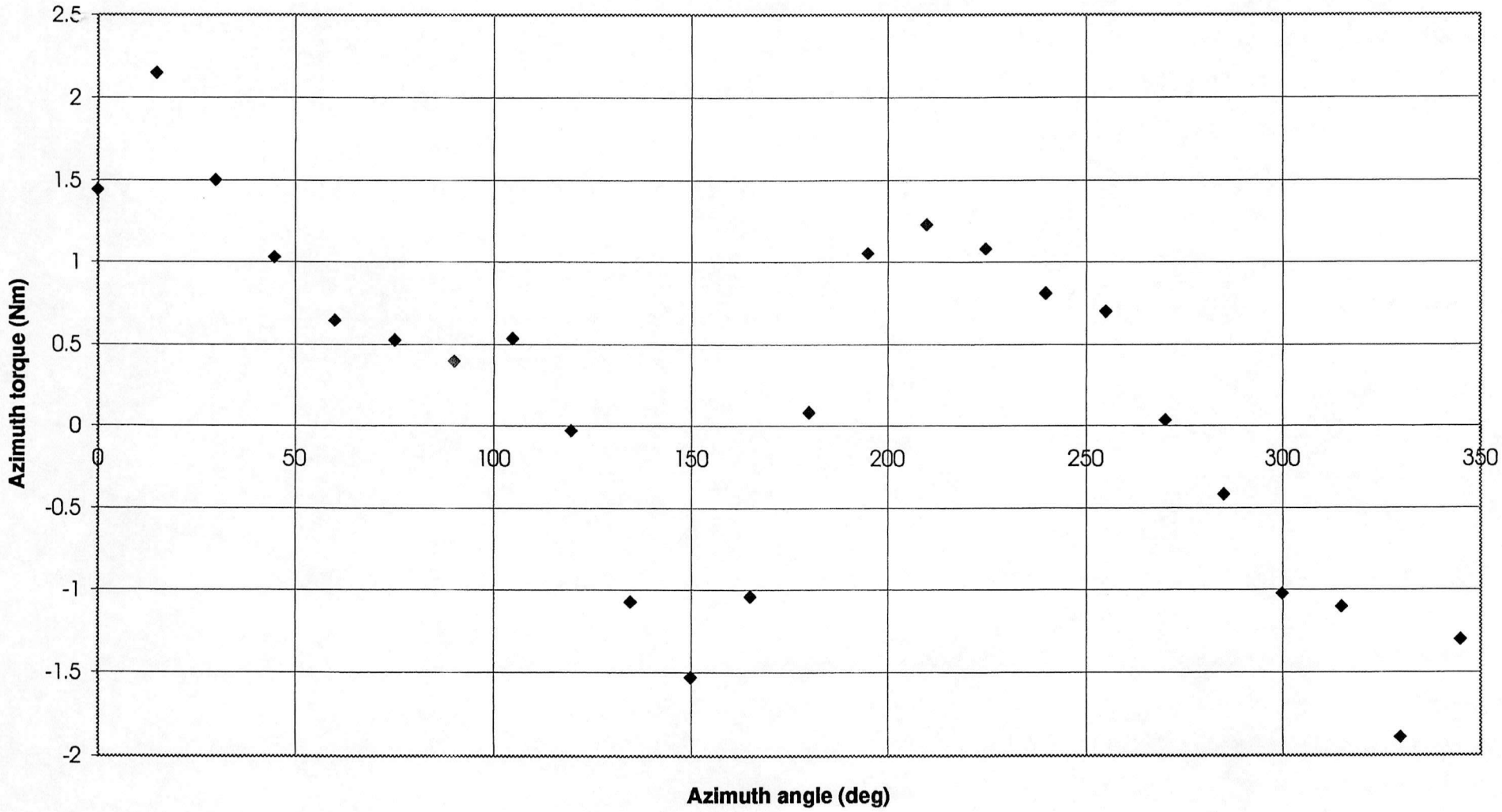

fig 10. SMALL TURRET: Elevation torque at elevation angle of 90 degrees

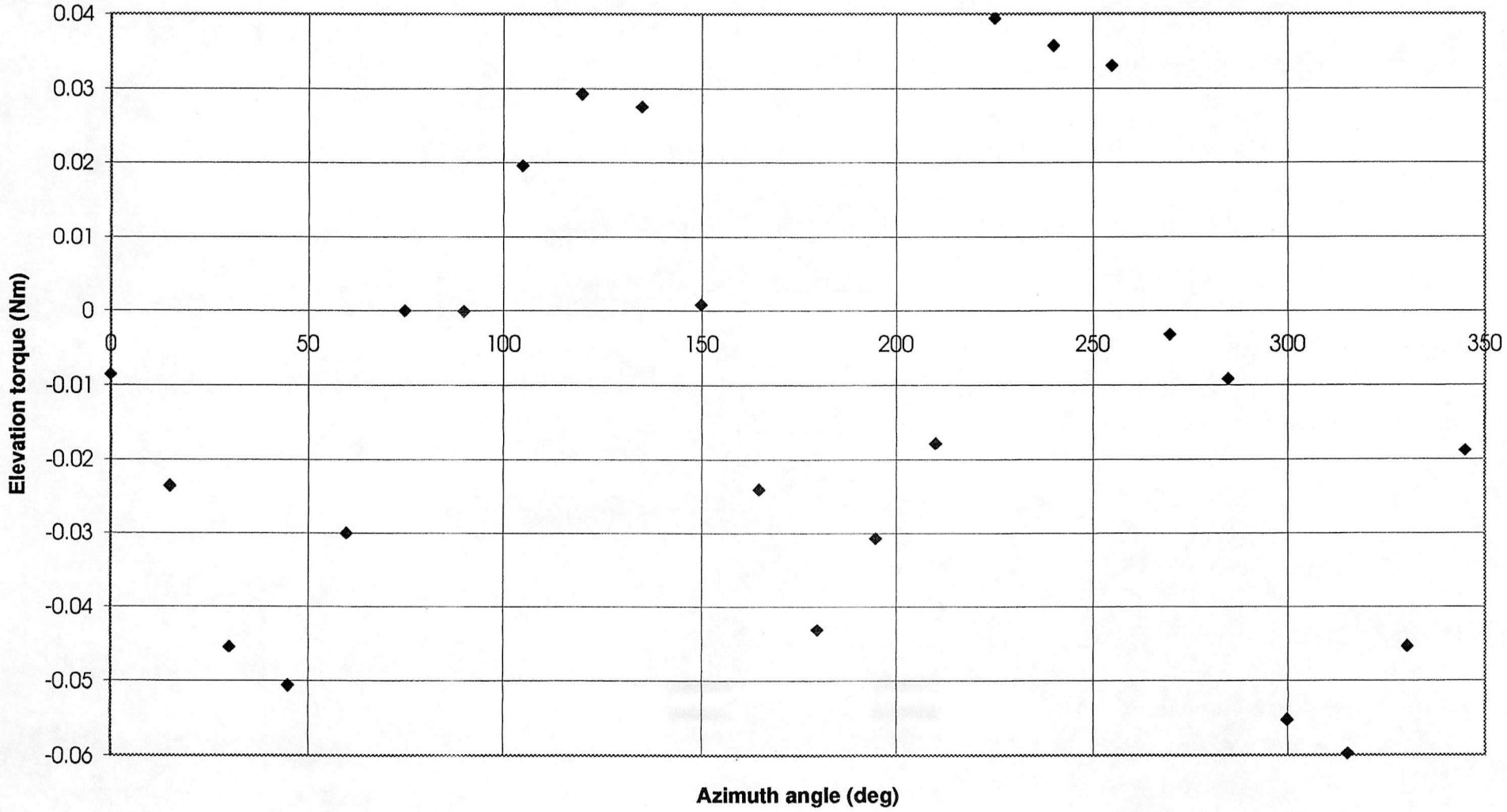

fig 11. SMALL TURRET: Azimuth torque standard deviation at elevation angle of 0 degrees

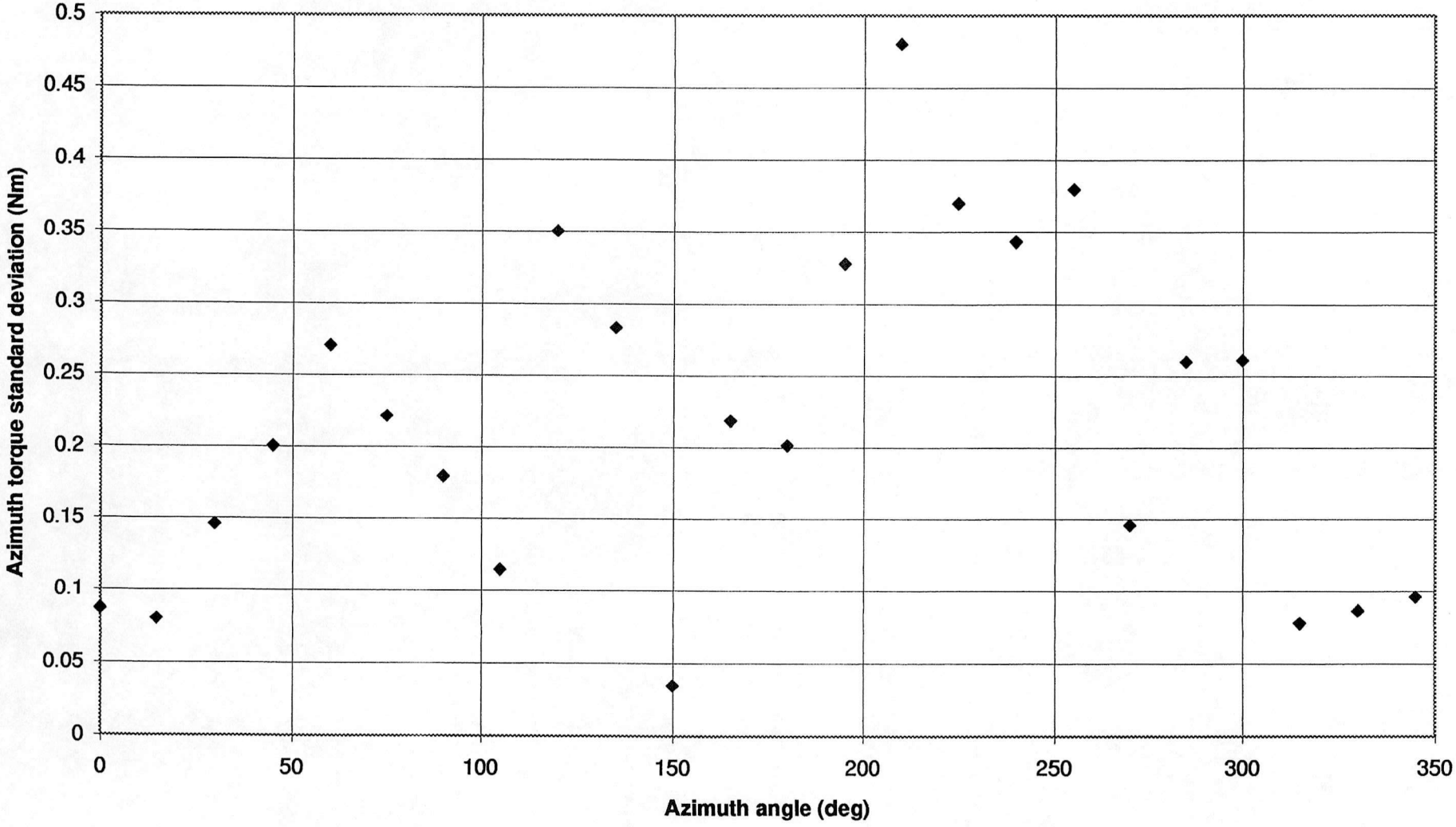

fig 12. SMALL TURRET: Elevation torque standard deviation at elevation angle of 0 degrees

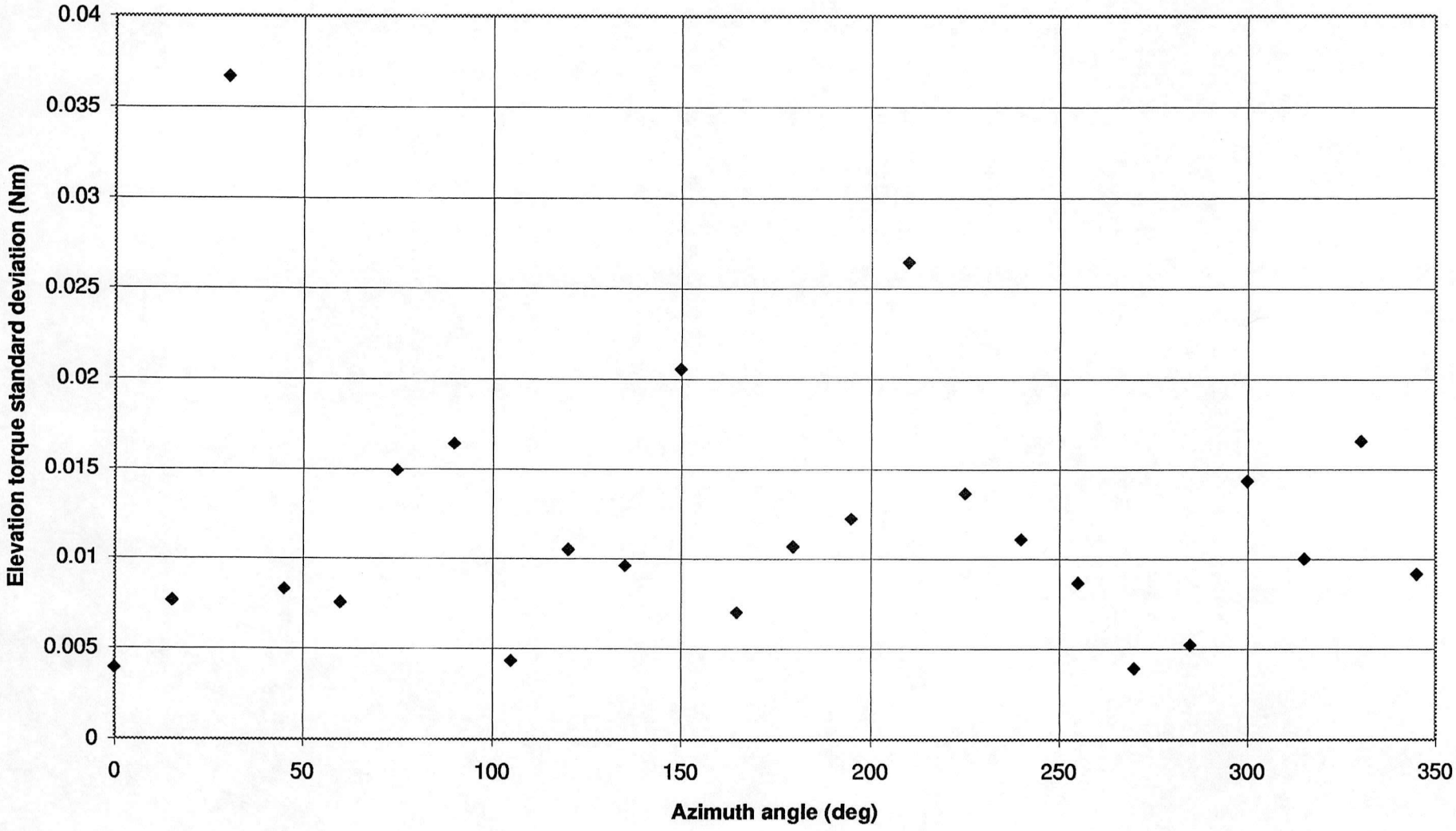

fig 13. SMALL TURRET: Azimuth torque standard deviation at elevation angle of -45 degrees

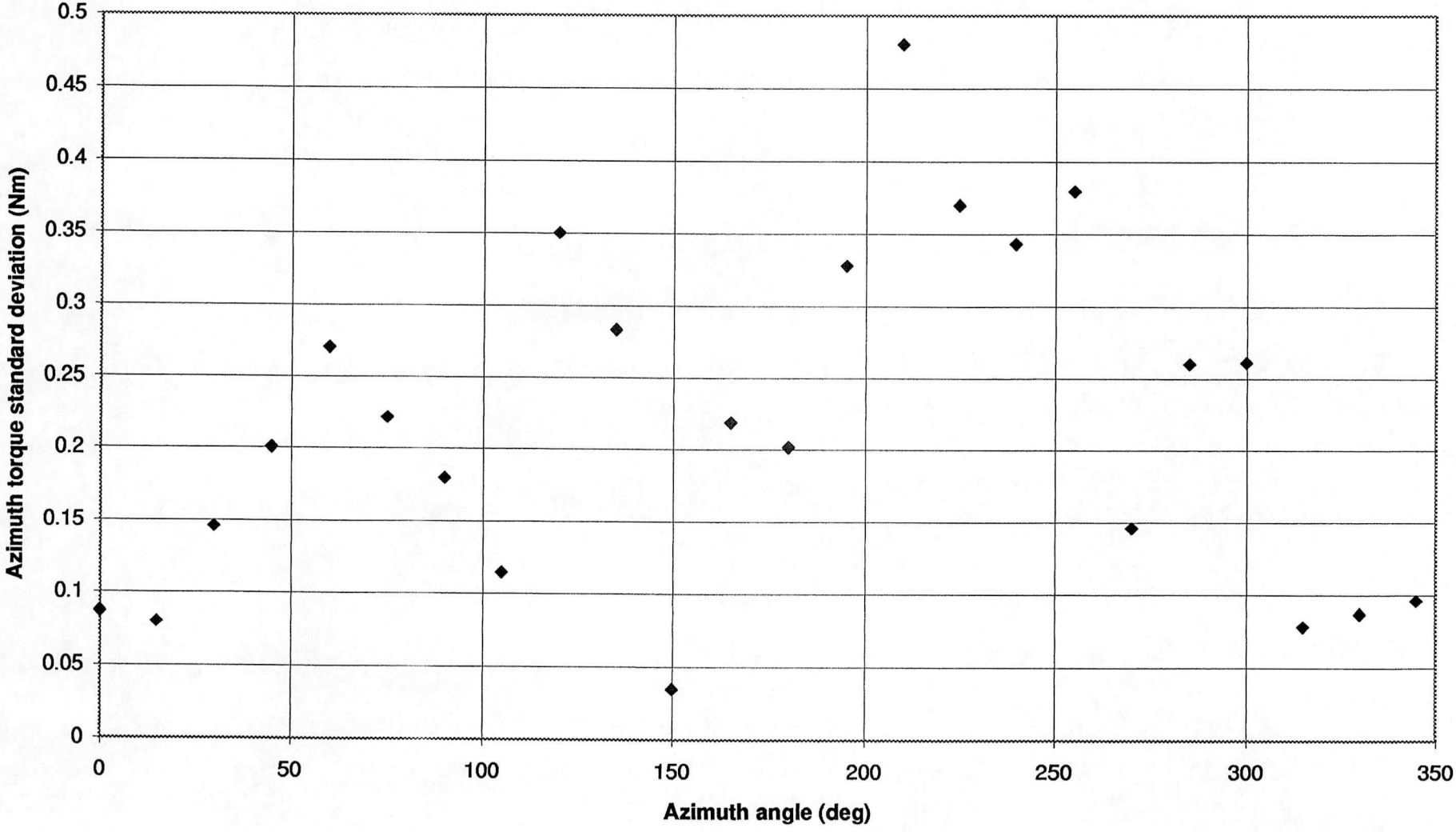

fig 14. SMALL TURRET: Elevation torque standard deviation at elevation angle of -45 degrees

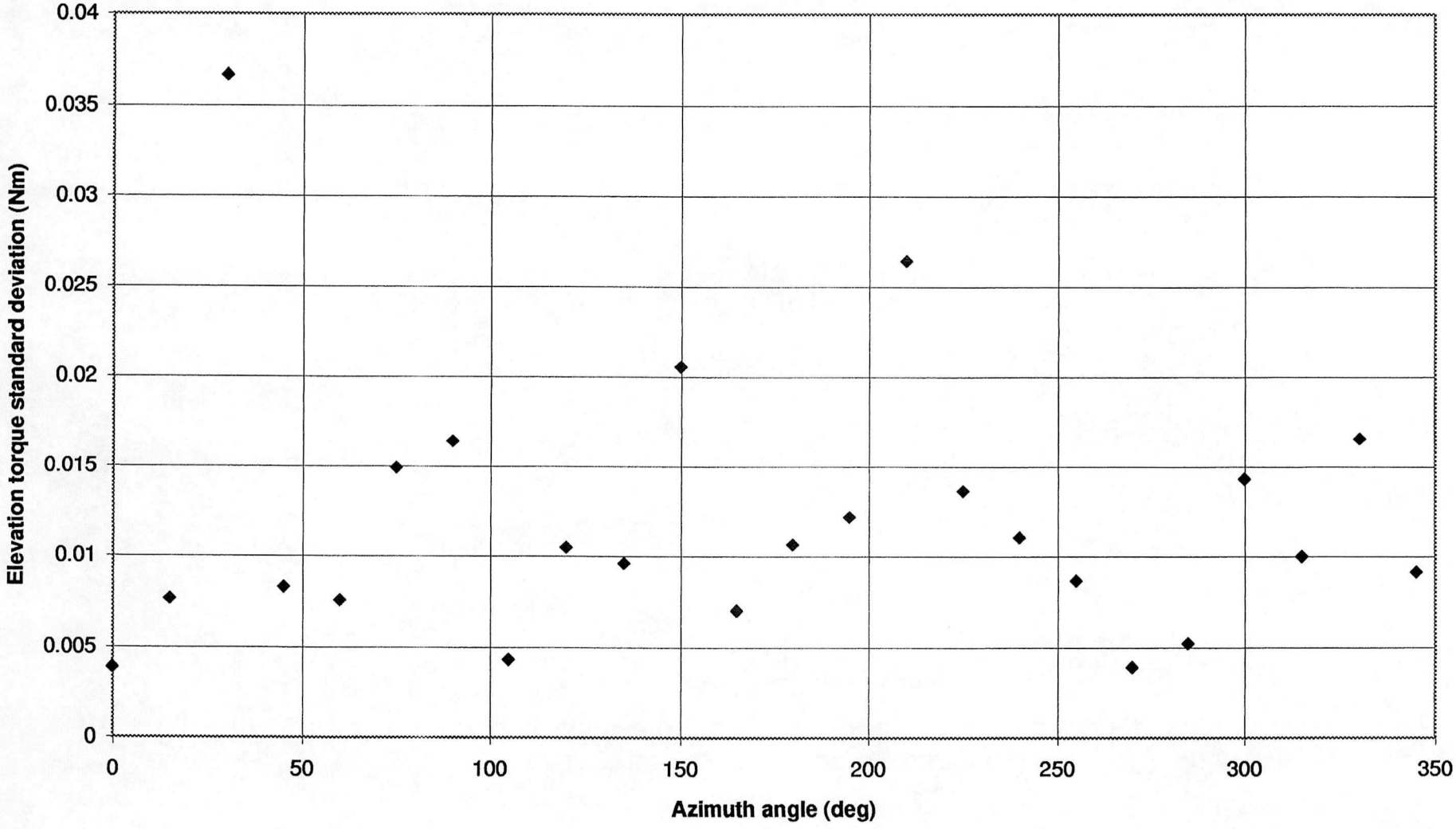

fig 15. SMALL TURRET: Azimuth torque standard deviation at elevation angle of -90 degrees

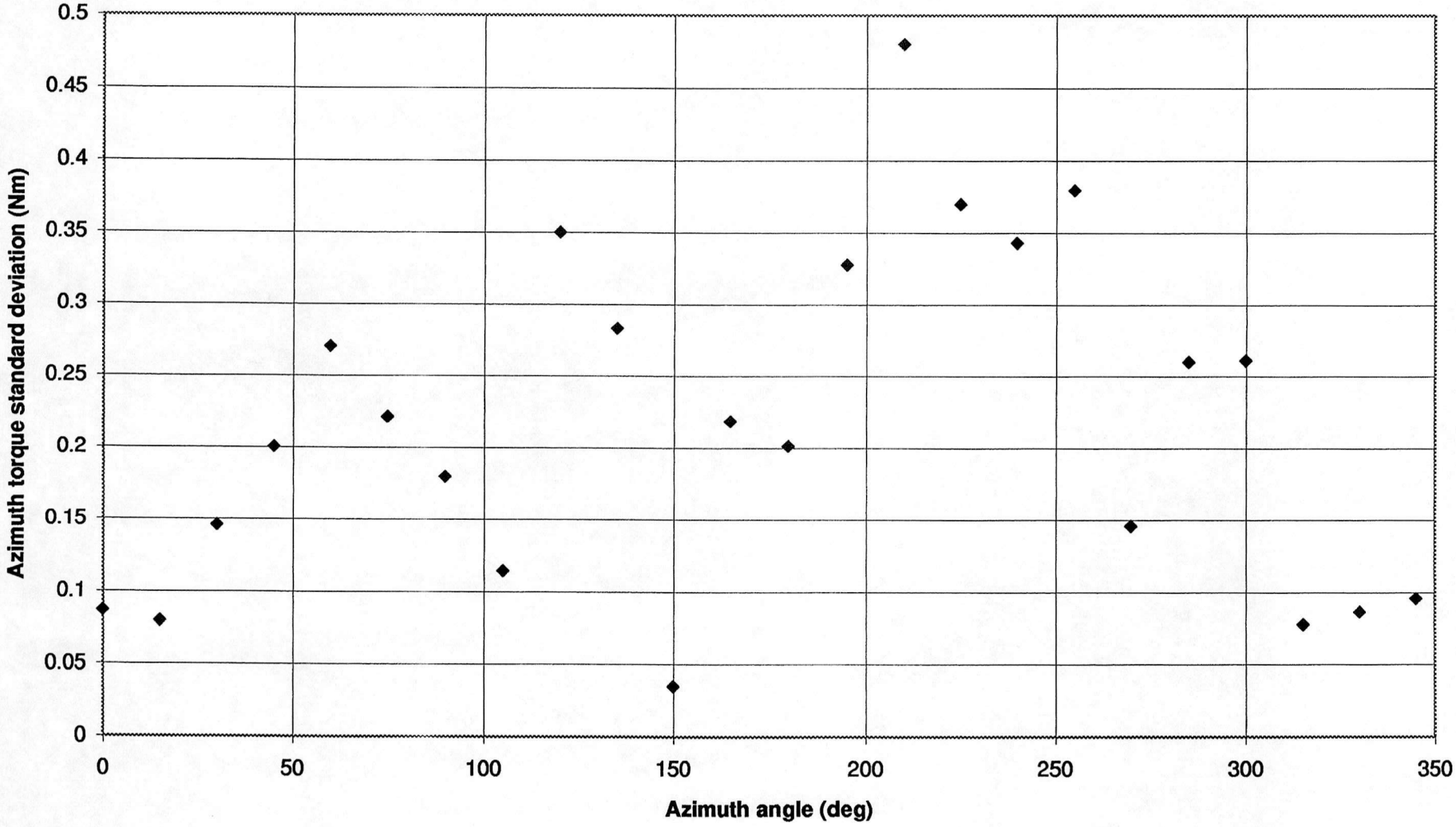

fig 16. SMALL TURRET: Elevation torque standard deviation at elevation angle of -90 degrees

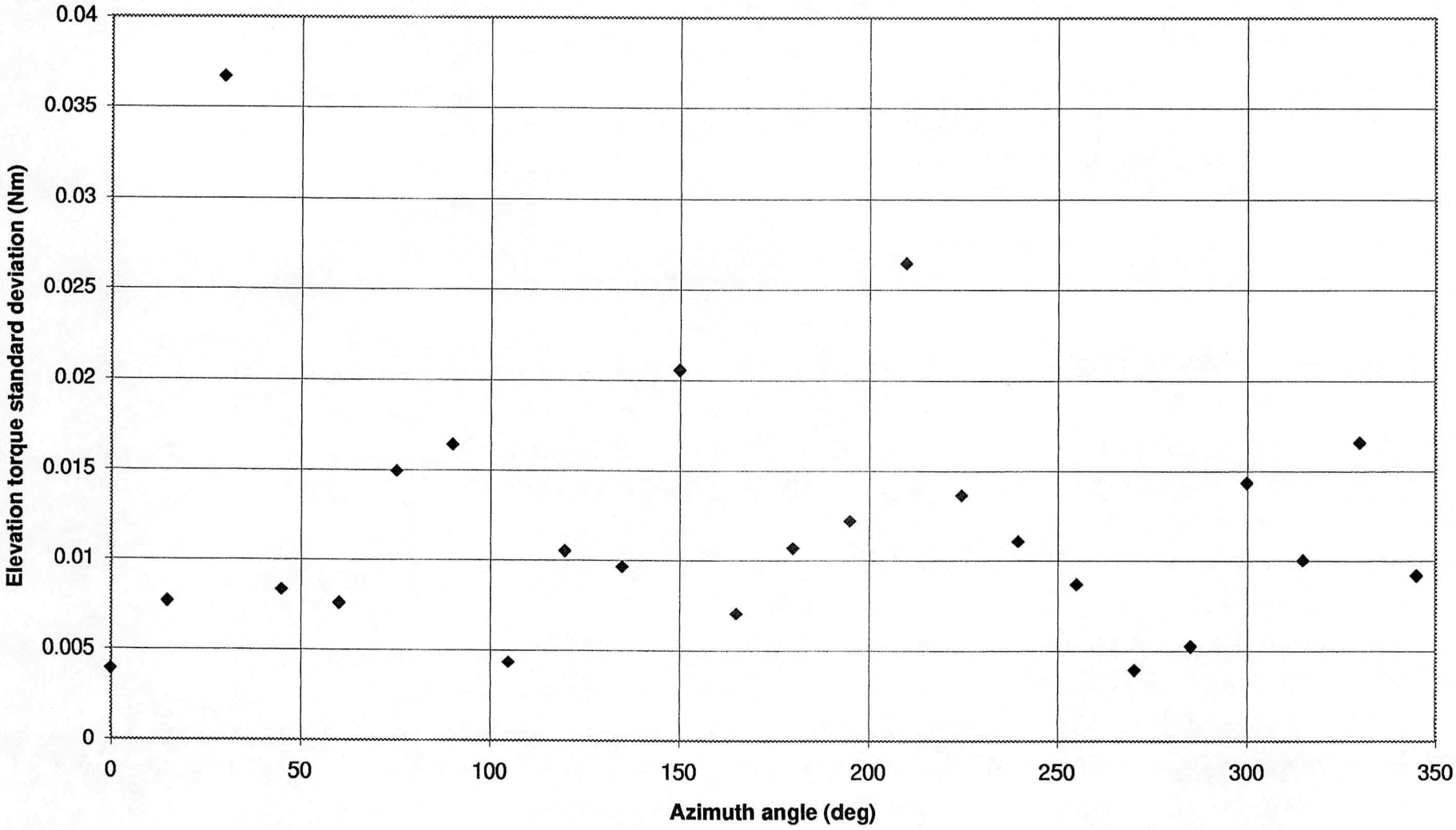

fig 17. SMALL TURRET: Azimuth torque standard deviation at elevation angle of 45 degrees

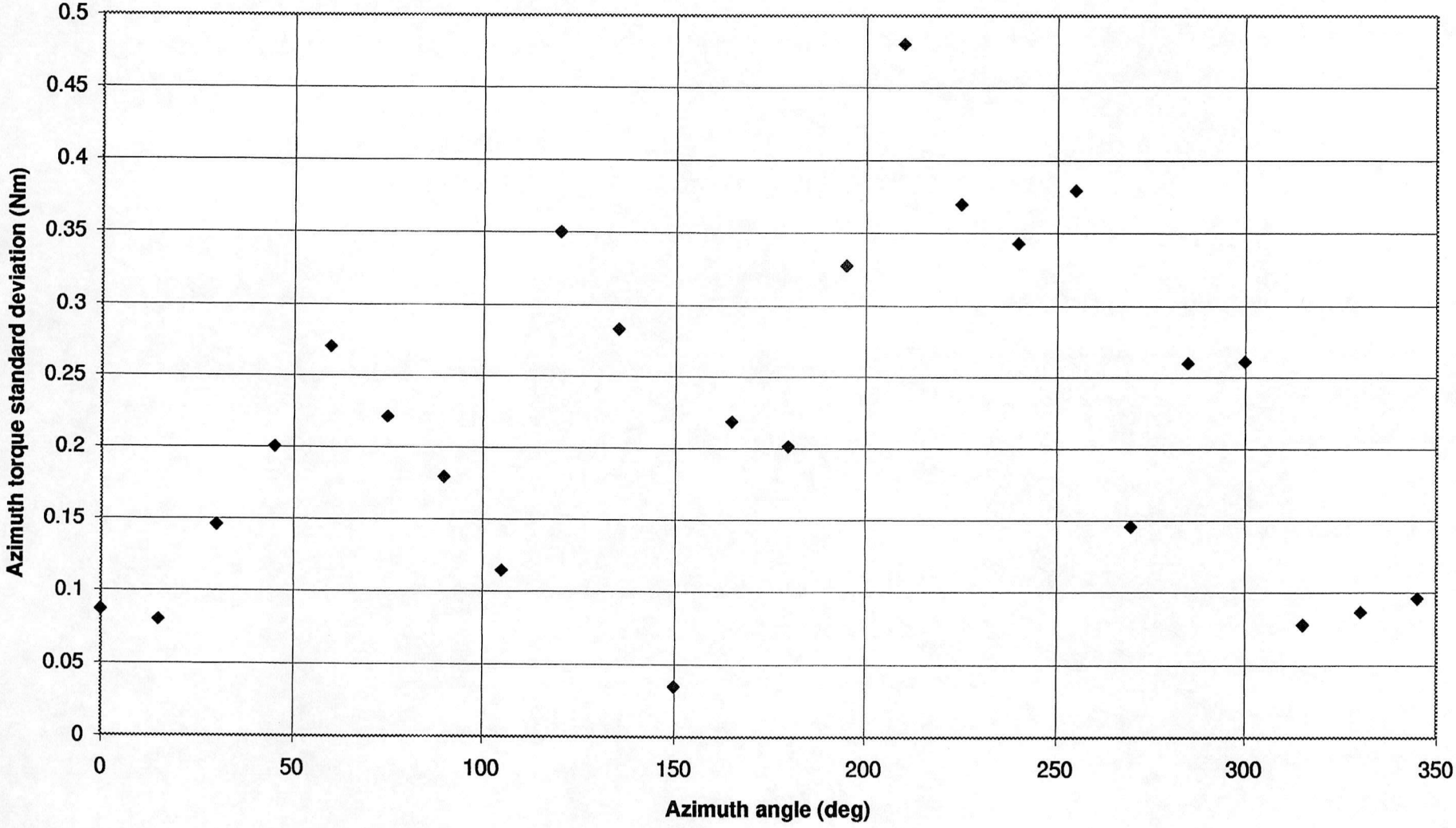

fig 18. SMALL TURRET: Elevation torque standard deviation at elevation angle of 45 degrees

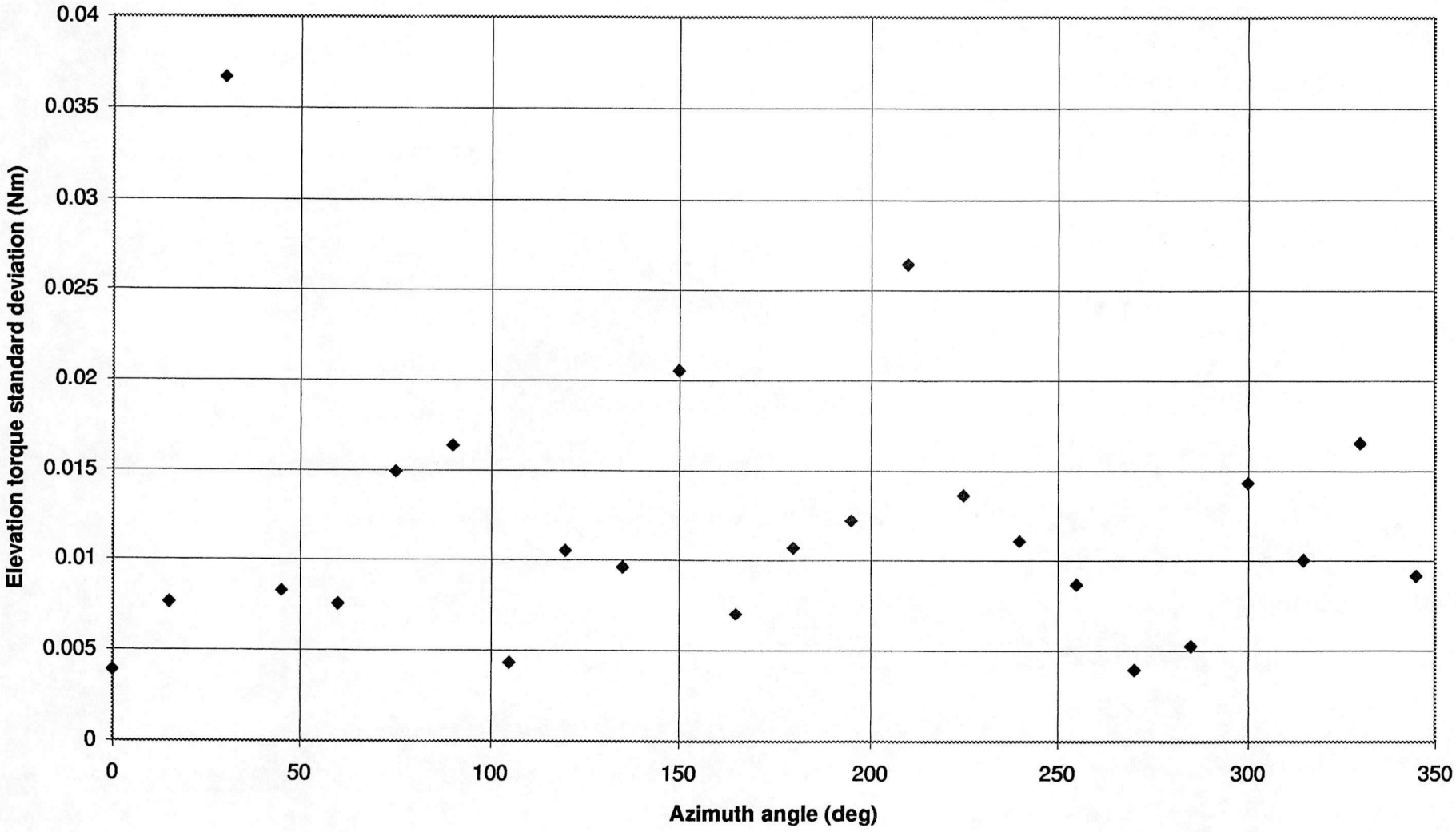

fig 19. SMALL TURRET: Azimuth torque standard deviation at elevation angle of 90 degrees

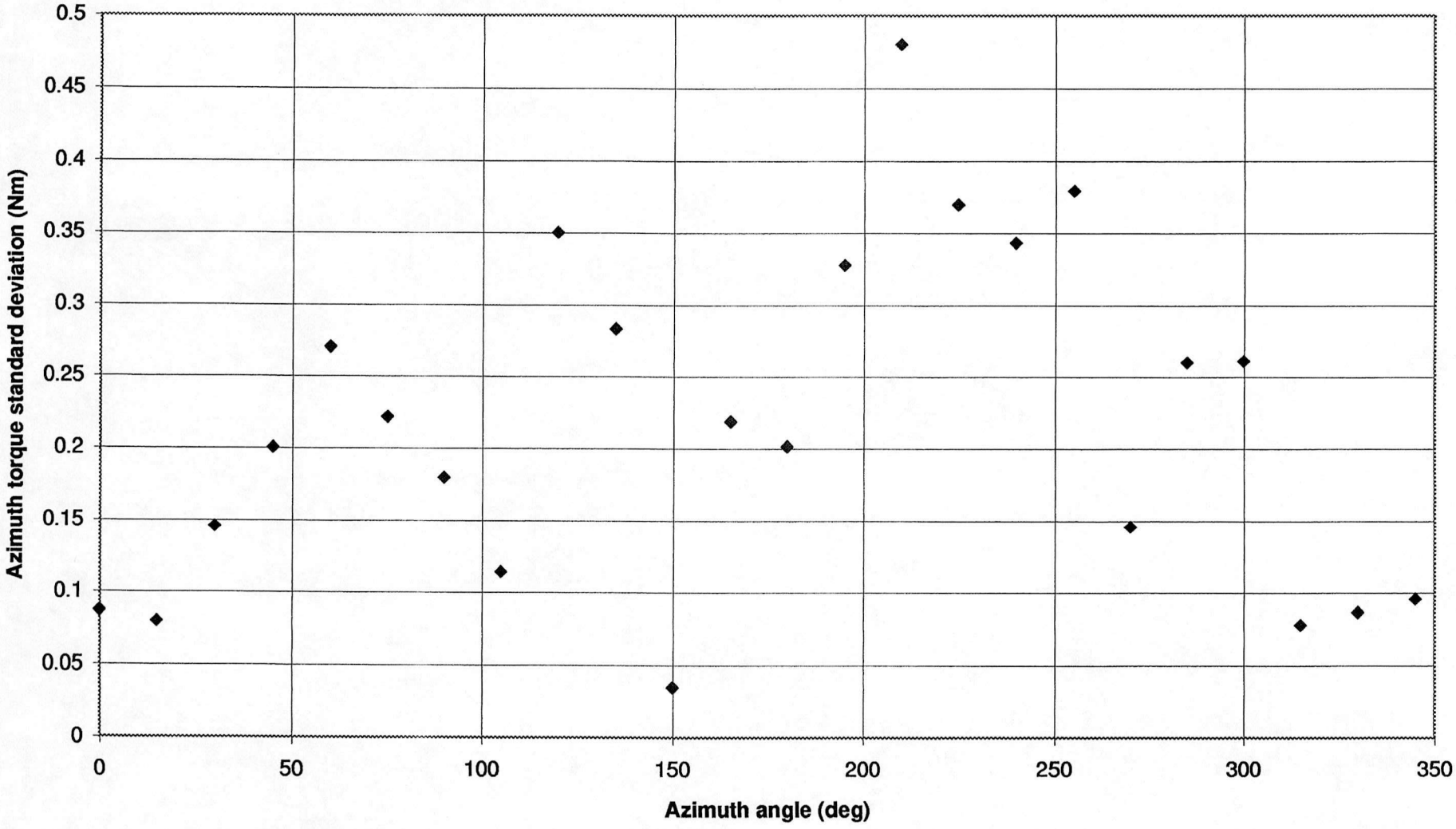

fig 20. SMALL TURRET: Elevation torque standard deviation at elevation angle of 90 degrees

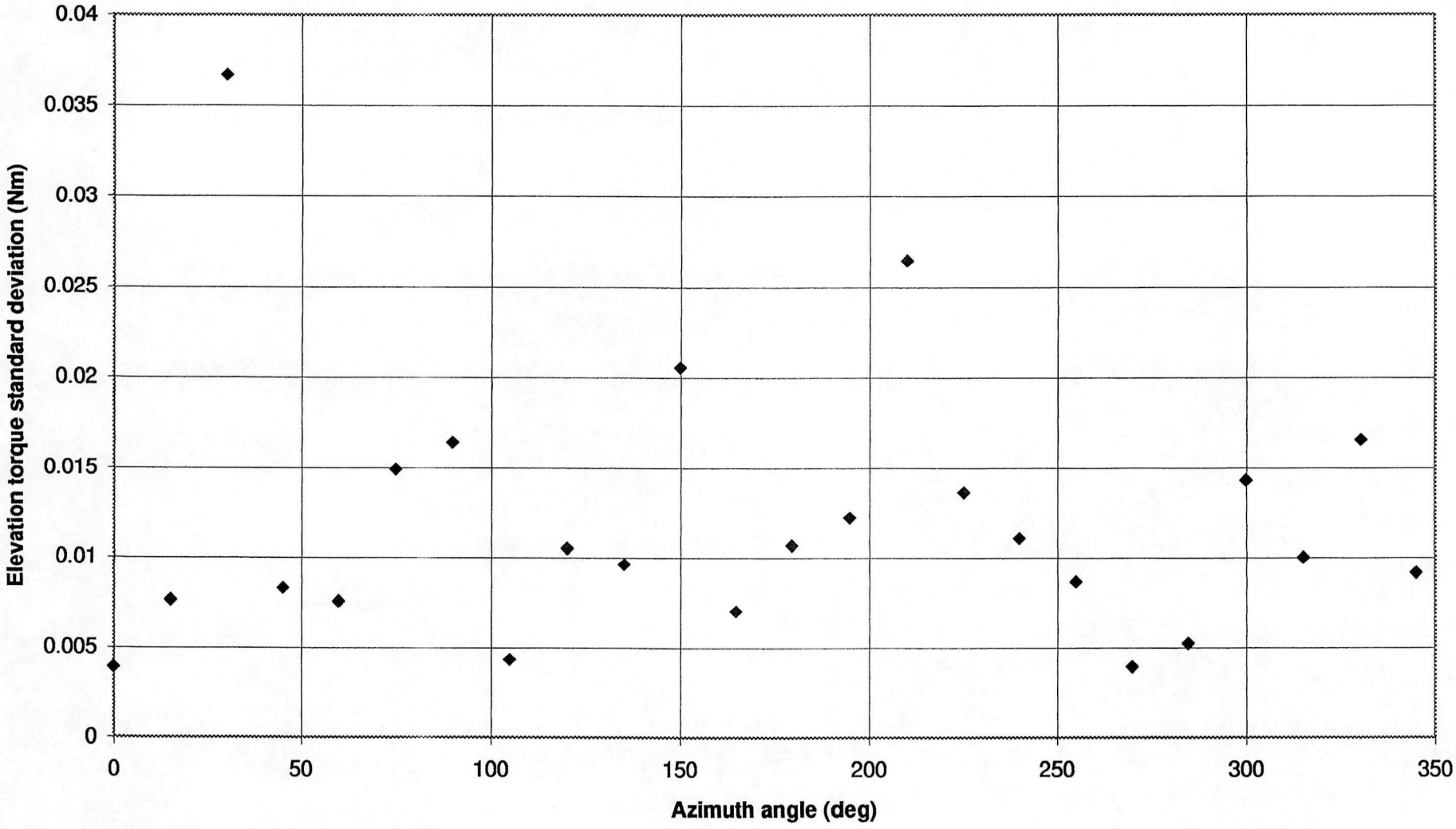

fig 21. LARGE TURRET: Azimuth torque at elevation angle of 0 degrees

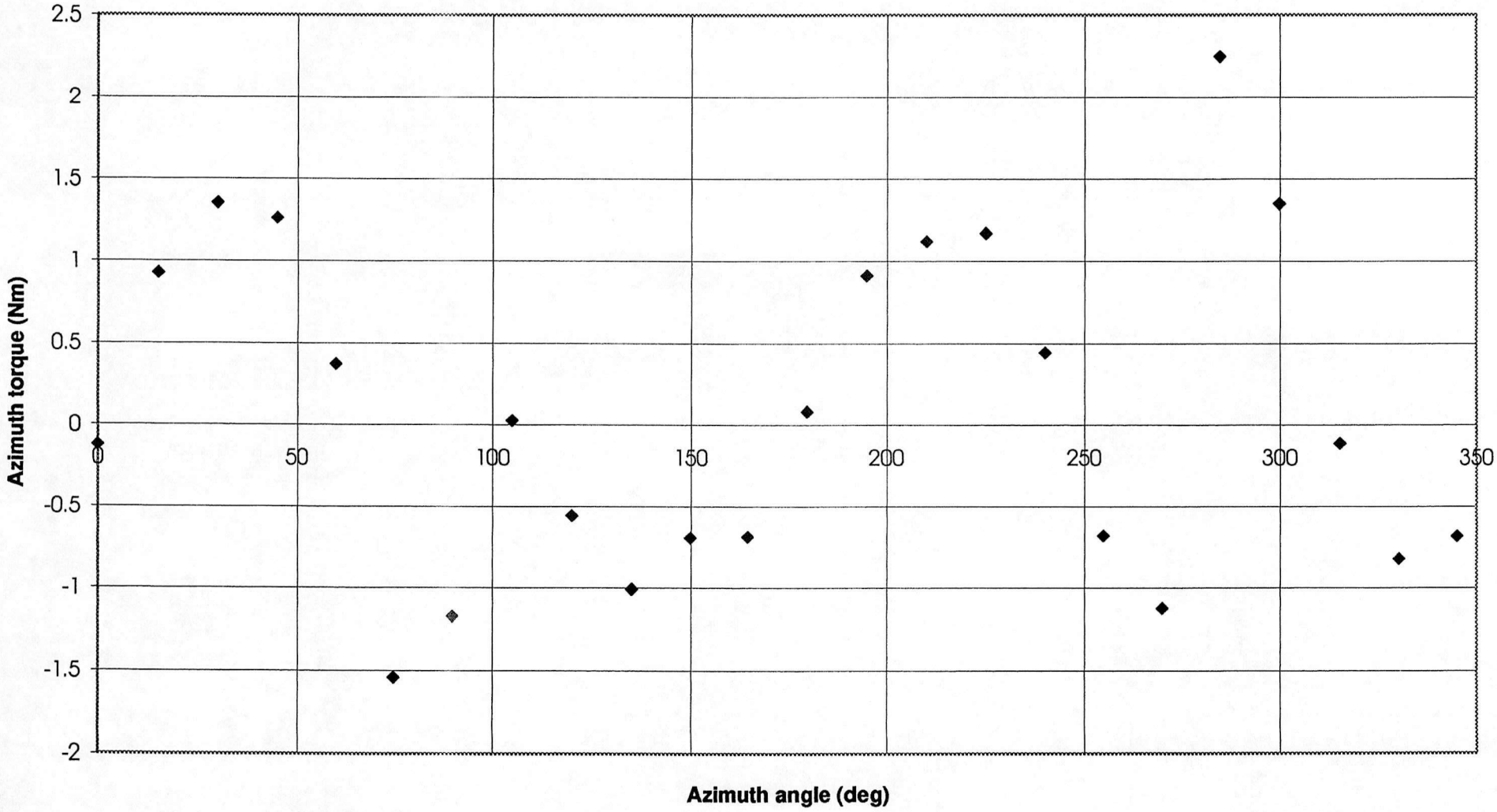

fig 22. LARGE TURRET: Elevation torque at elevation angle of 0 degrees

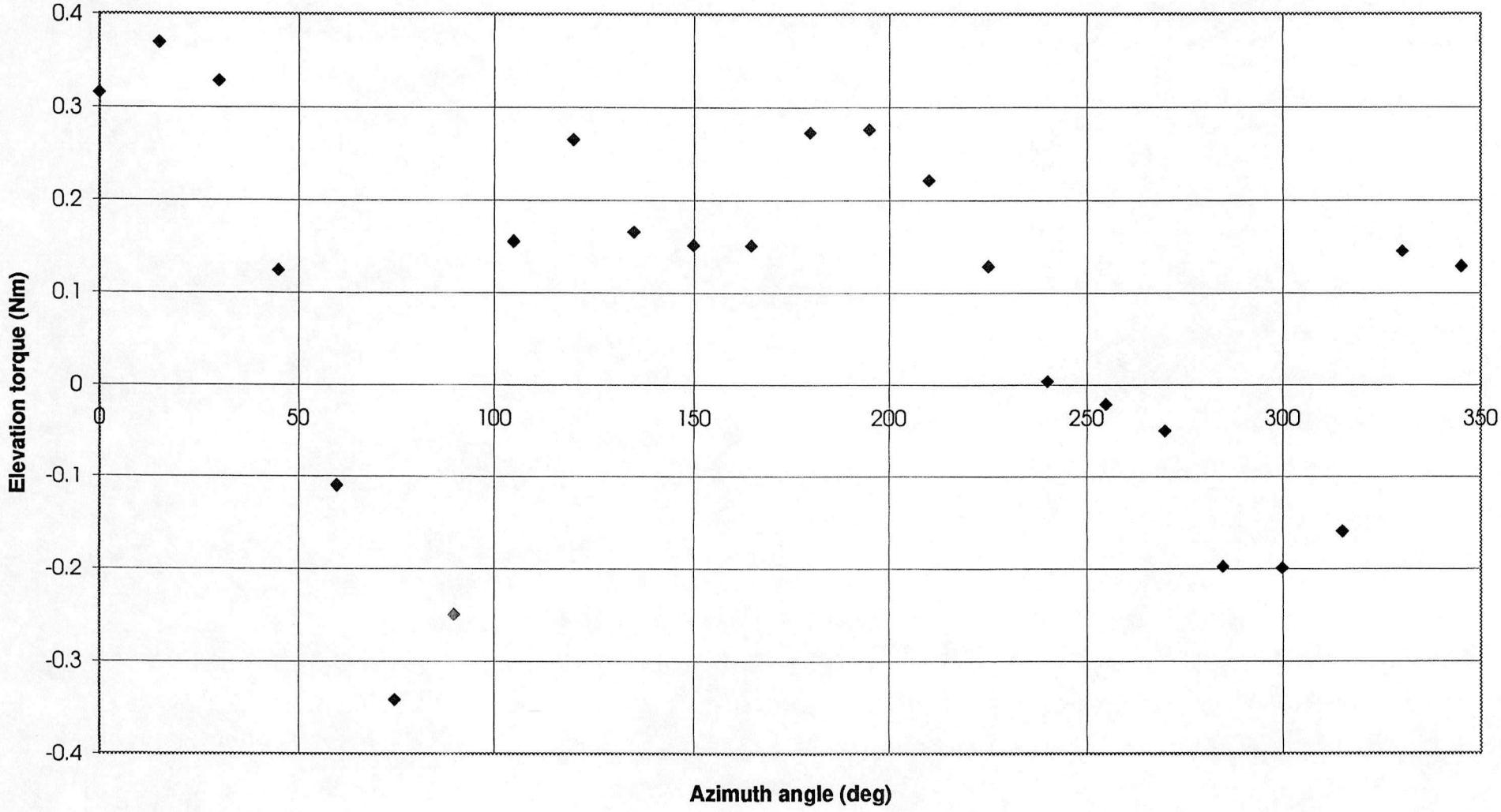

fig 23. LARGE TURRET: Azimuth torque at elevation angle of -45 degrees

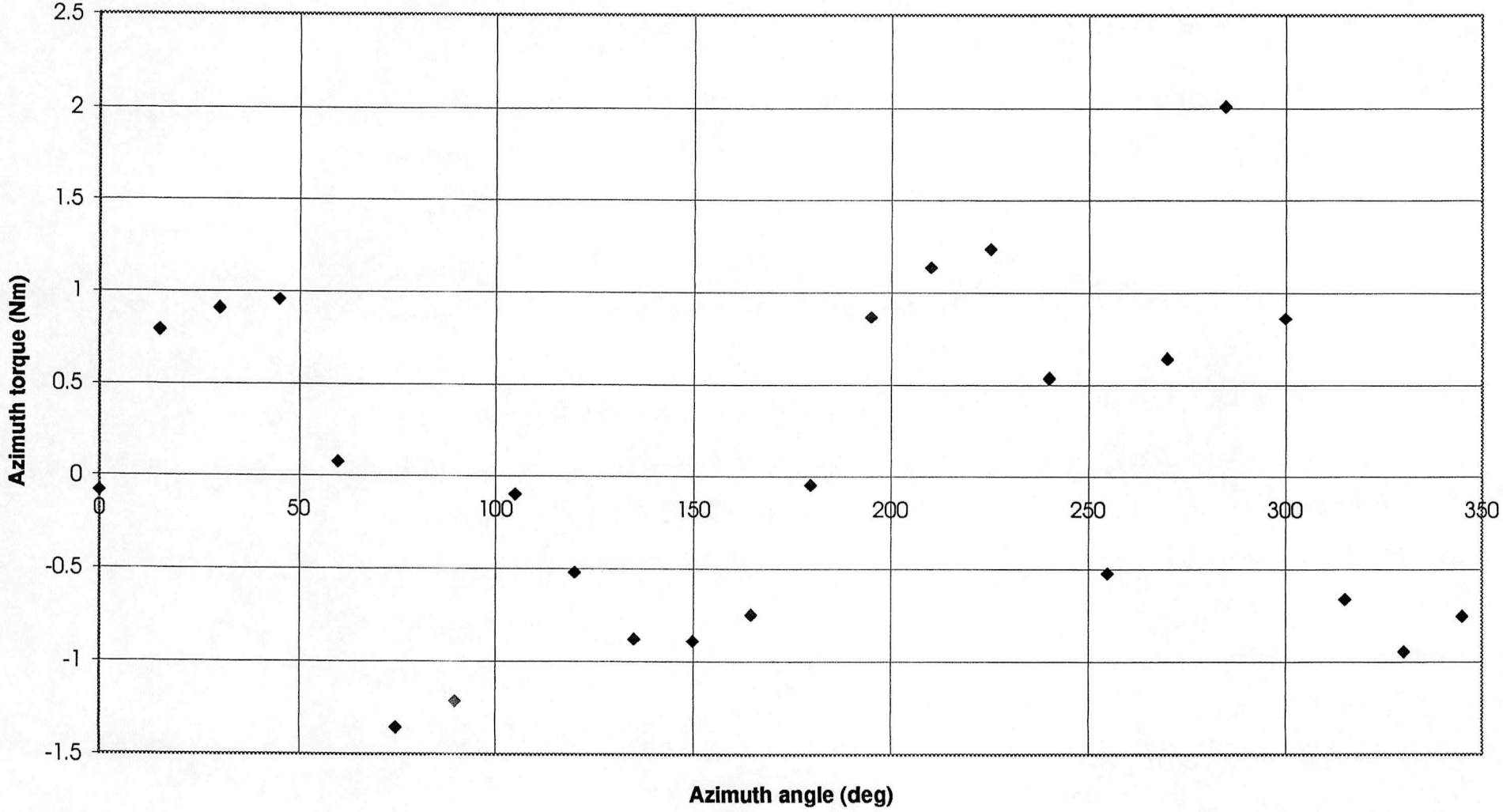

fig 24. LARGE TURRET: Elevation torque at elevation angle of -45 degrees

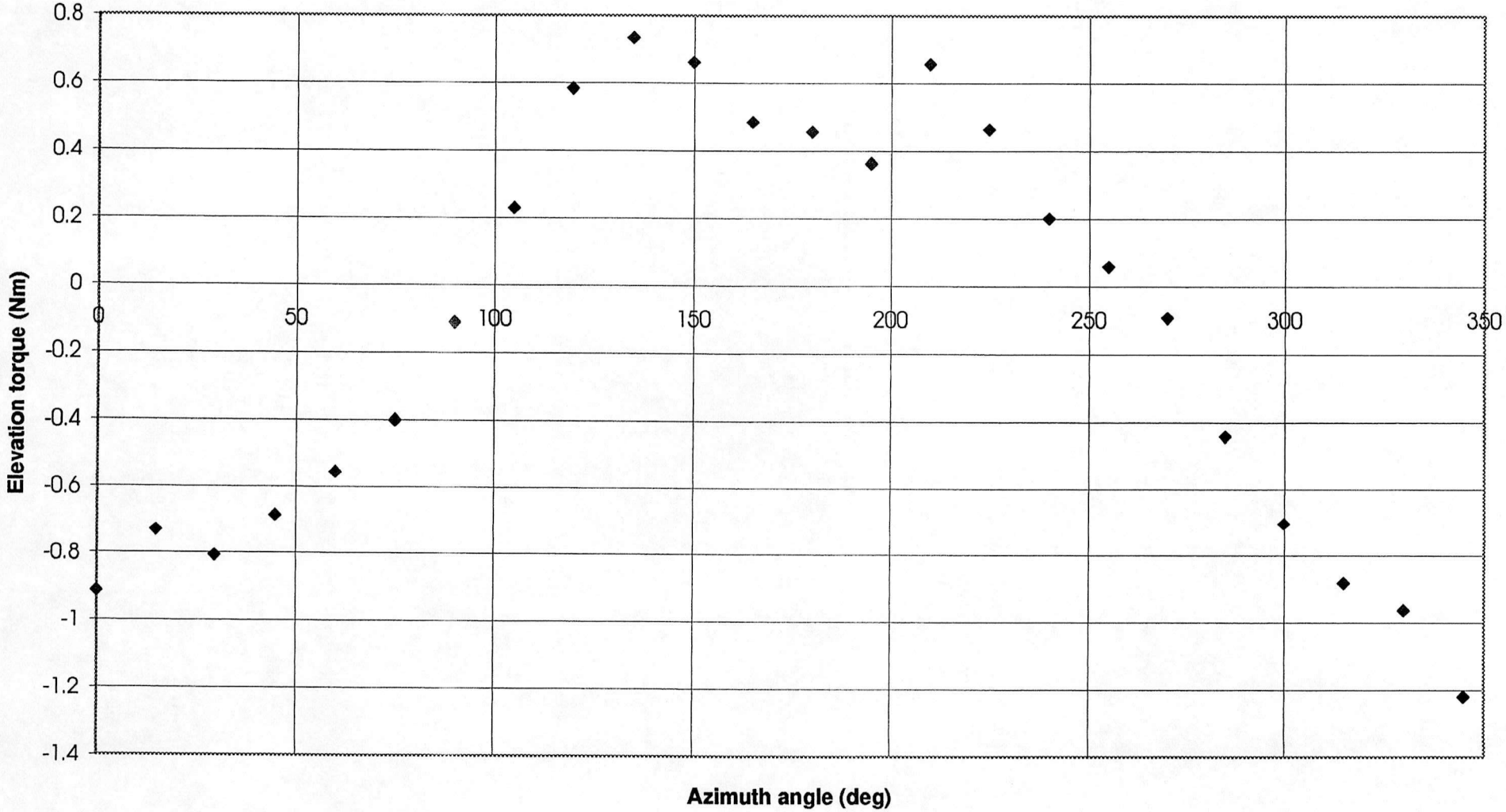

fig 25. LARGE TURRET: Azimuth torque at elevation angle of -90 degrees

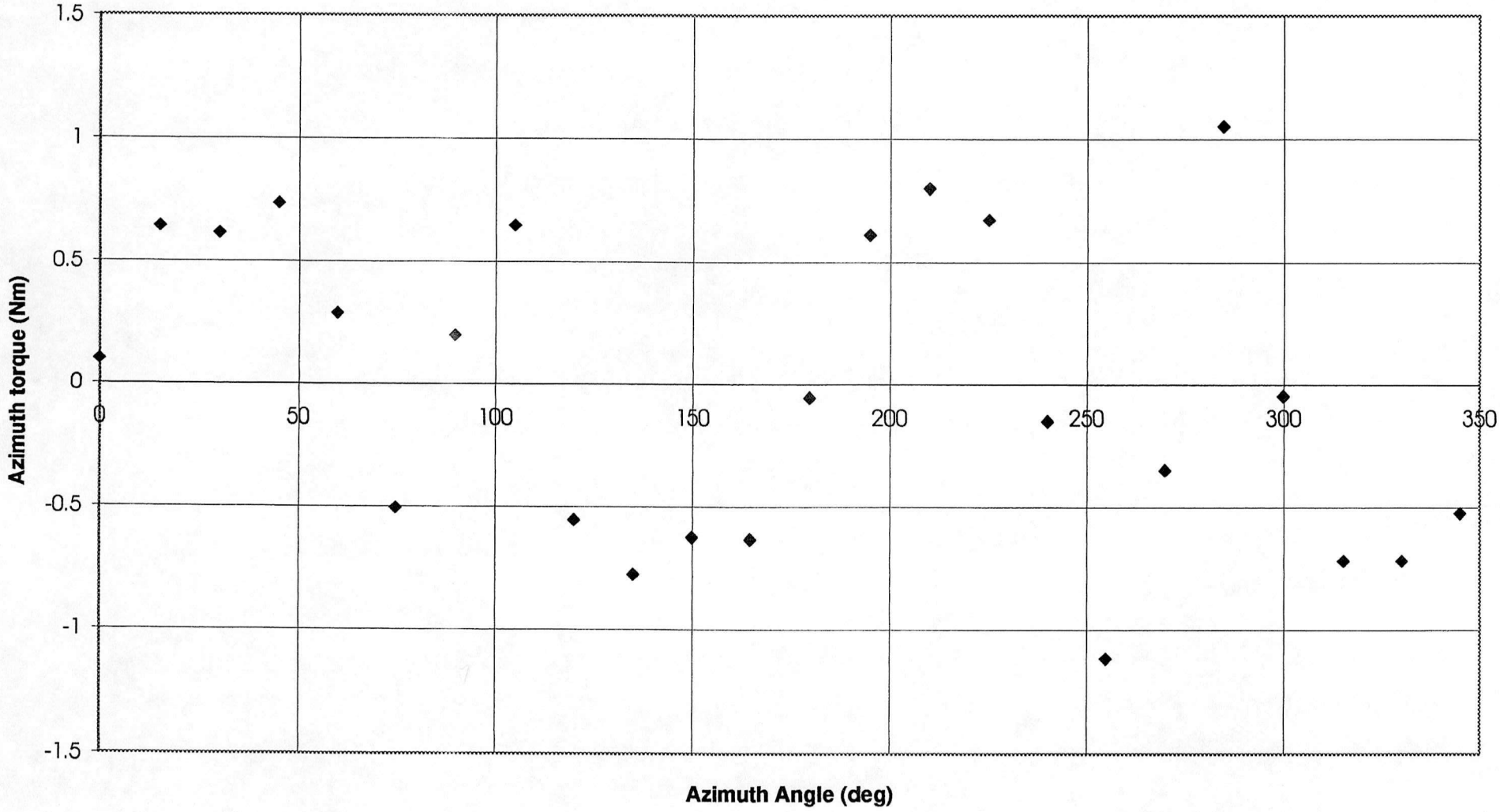

fig 26. LARGE TURRET: Elevation torque at elevation angle of -90 degrees

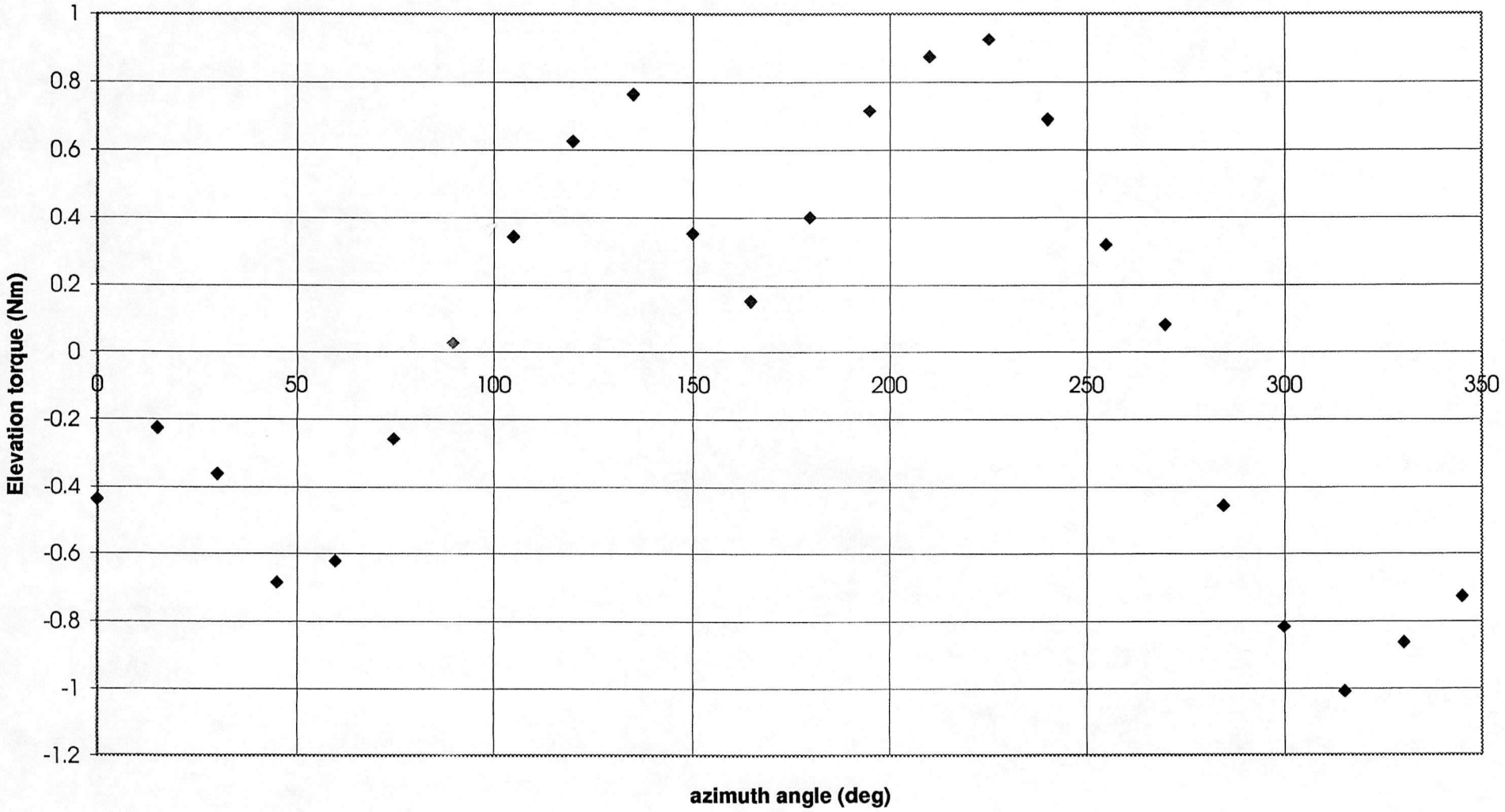

fig 27. LARGE TURRET: Azimuth torque at elevation angle of 45 degrees

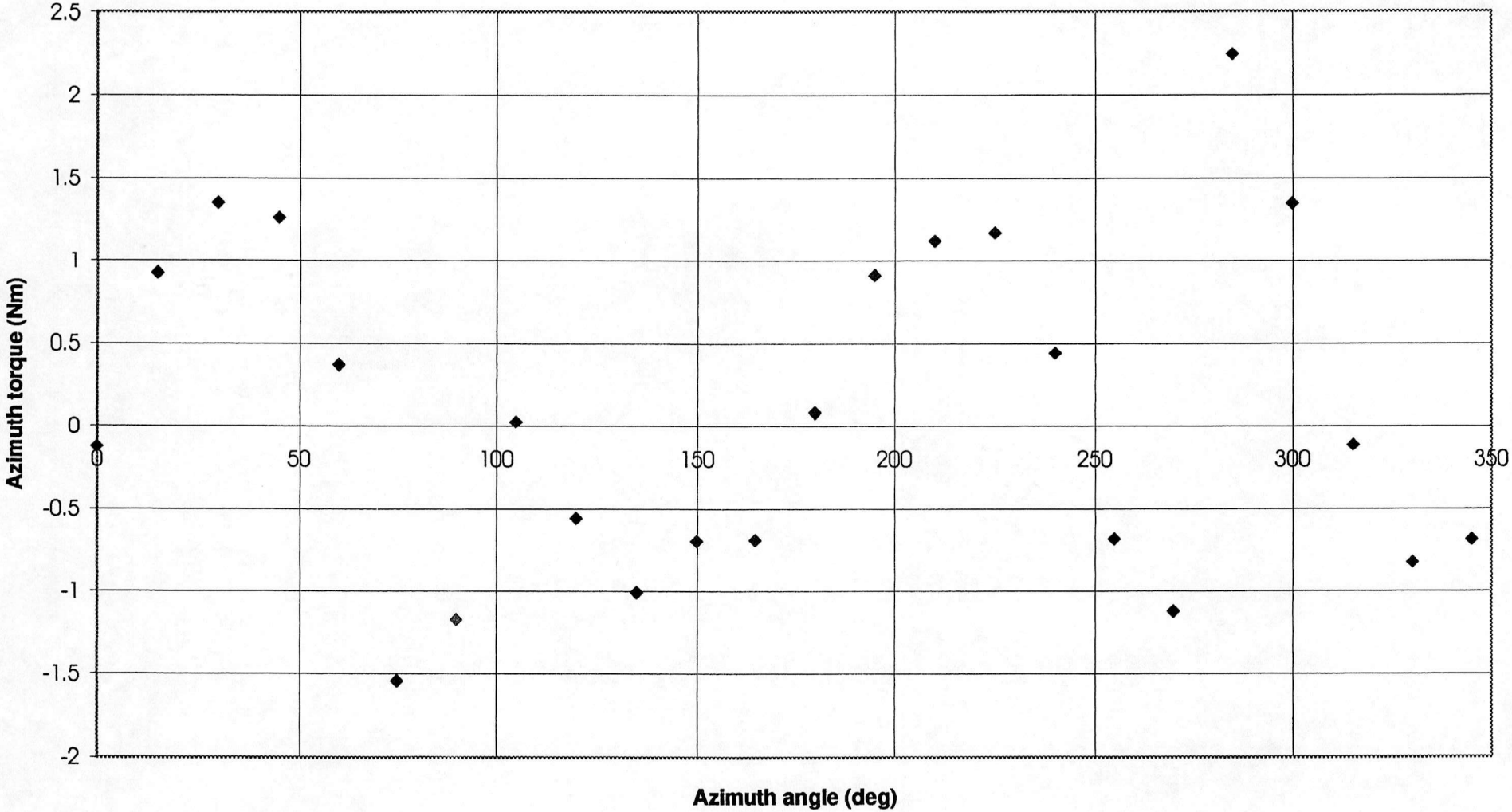

fig 28. LARGE TURRET: Elevation torque at elevation angle of 45 degrees

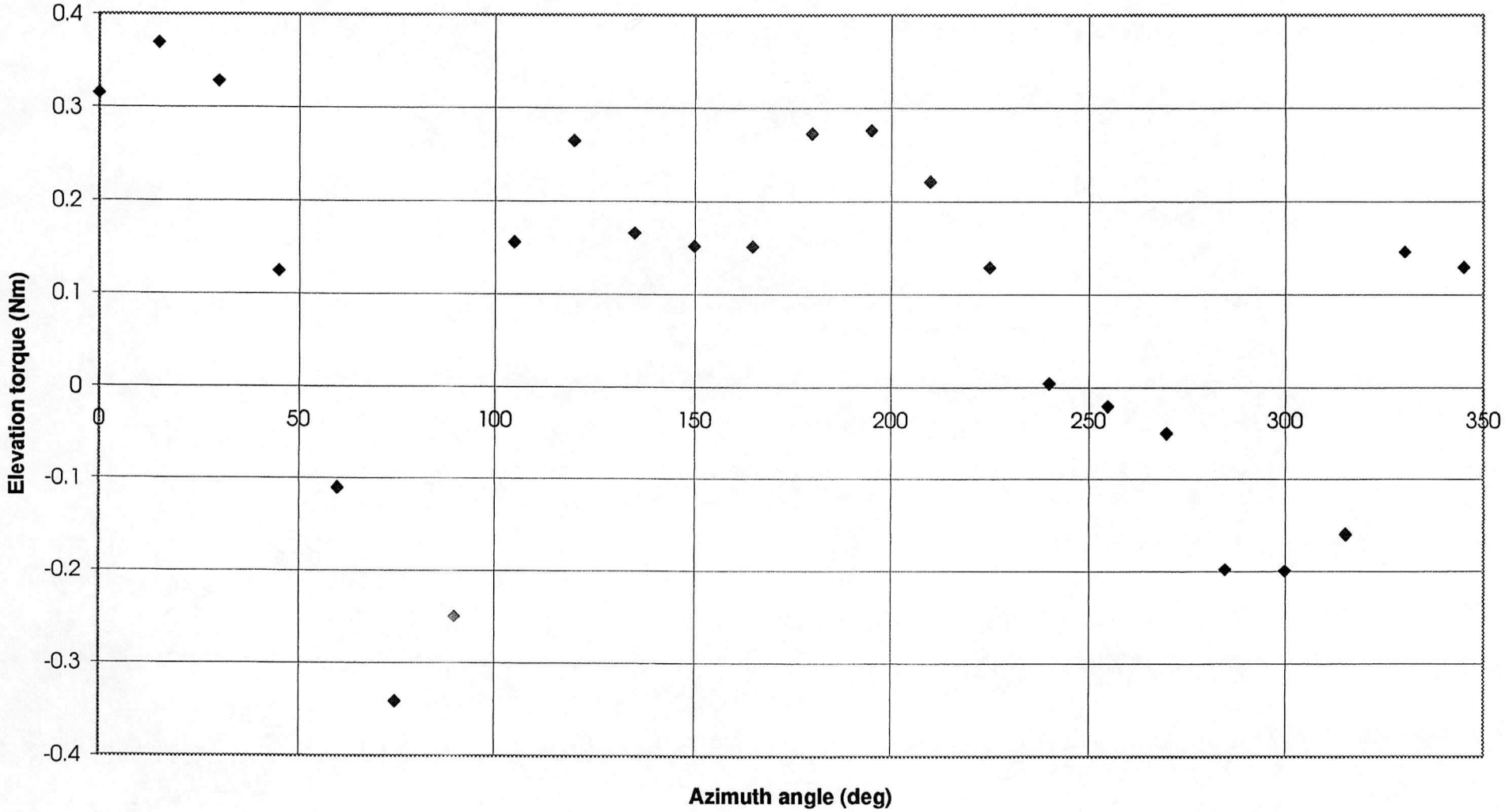

fig 29. LARGE TURRET: Azimuth torque at elevation angle of 90 degrees

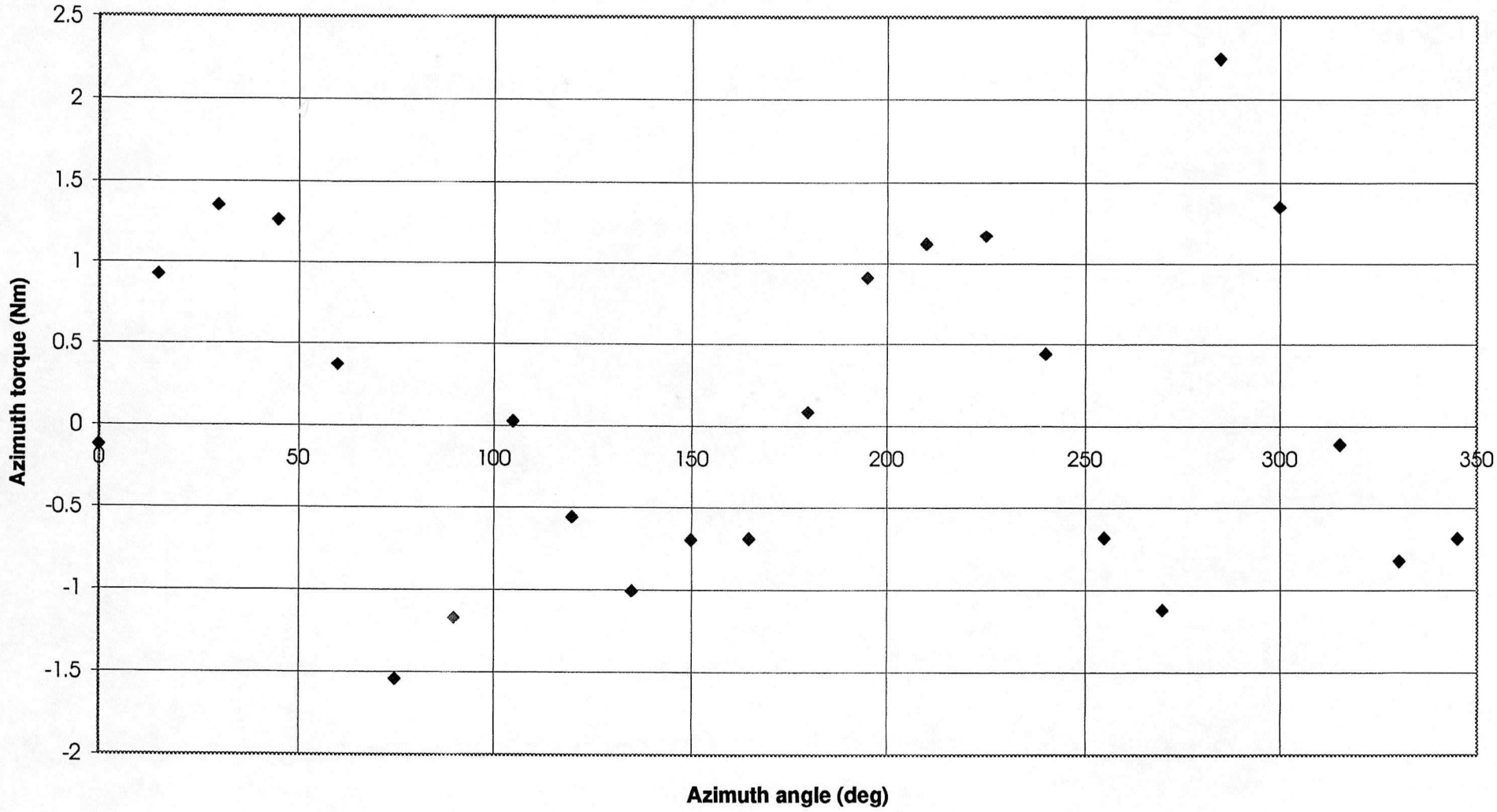

fig 30. LARGE TURRET: Elevation torque at elevation angle of 90 degrees

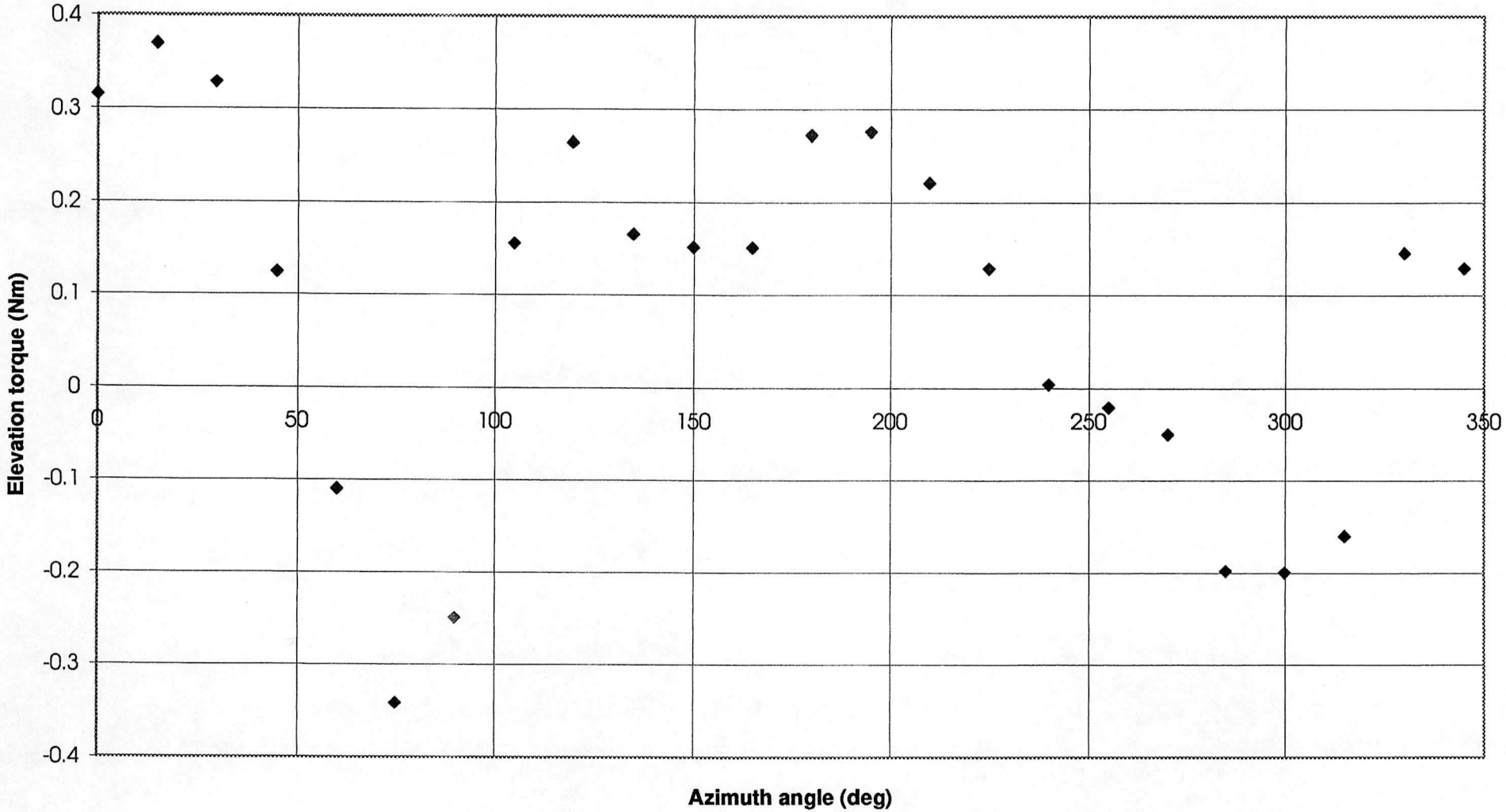

Fig 31. LARGE TURRET: Azimuth torque standard deviation at elevation angle of 0 degrees

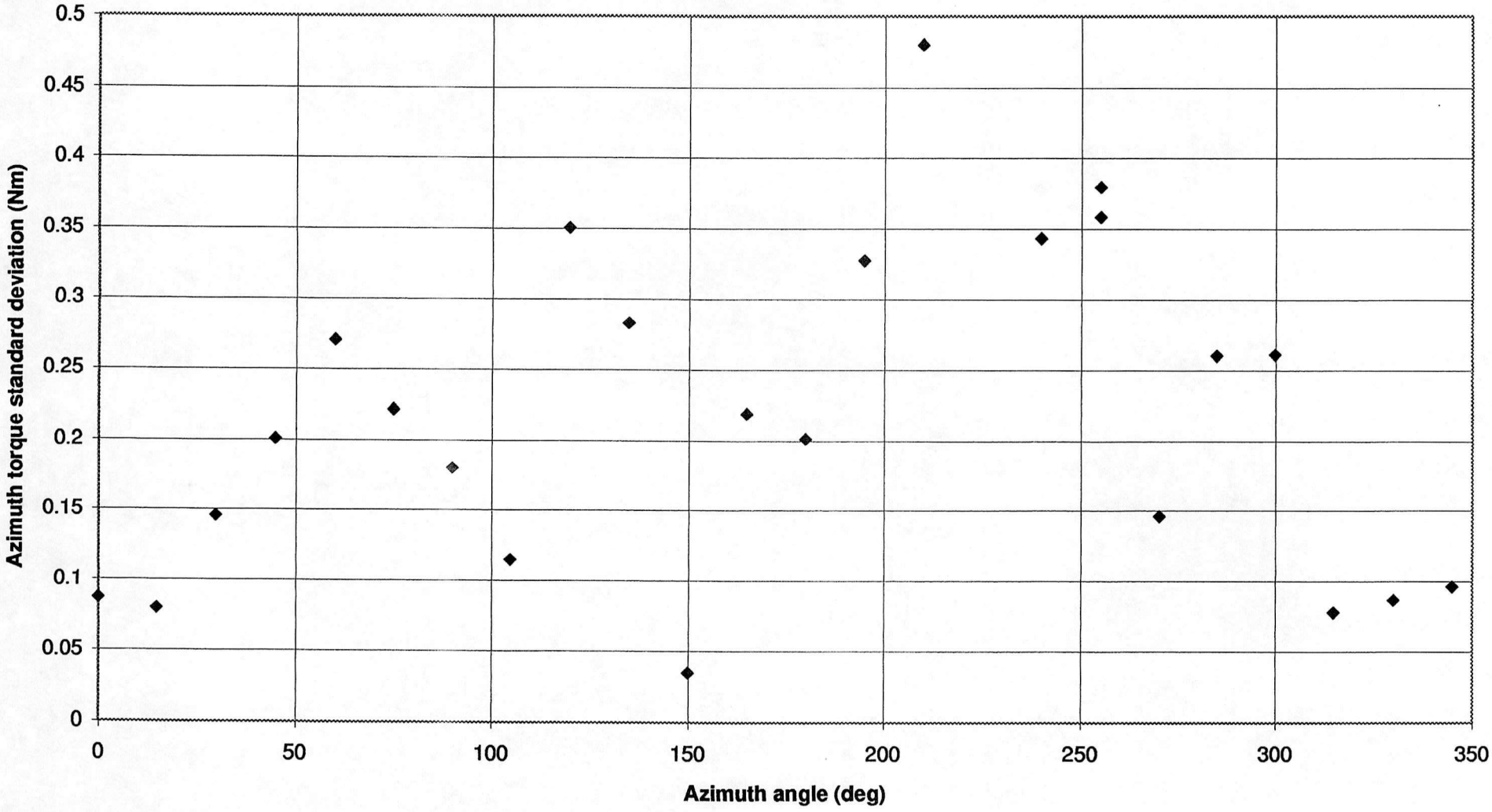

Fig 32. LARGE TURRET: Elevation torque standard deviation at elevation angle of 0 degrees

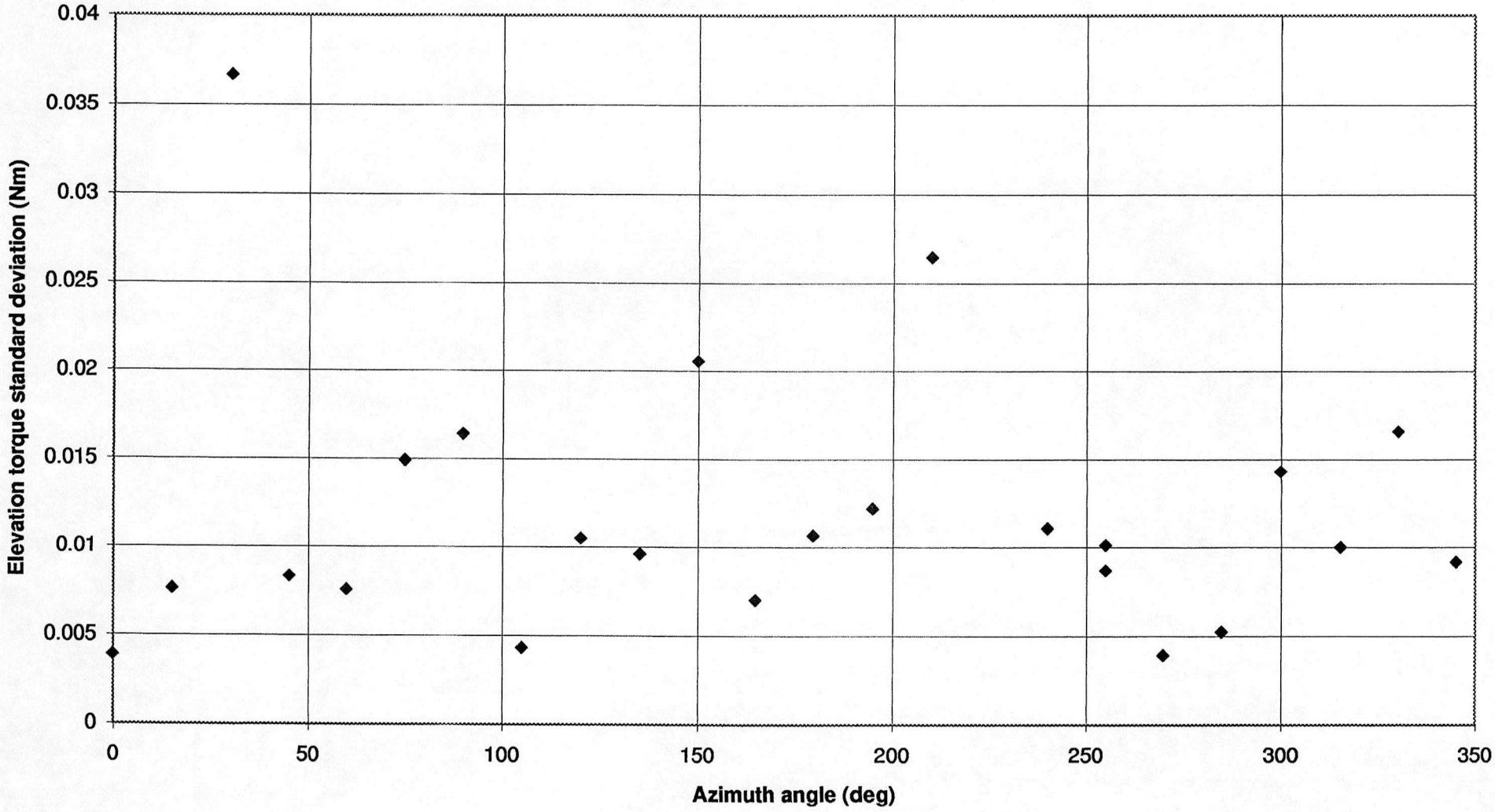

Fig 33. LARGE TURRET: Azimuth torque standard deviation at elevation angle of -45 degrees

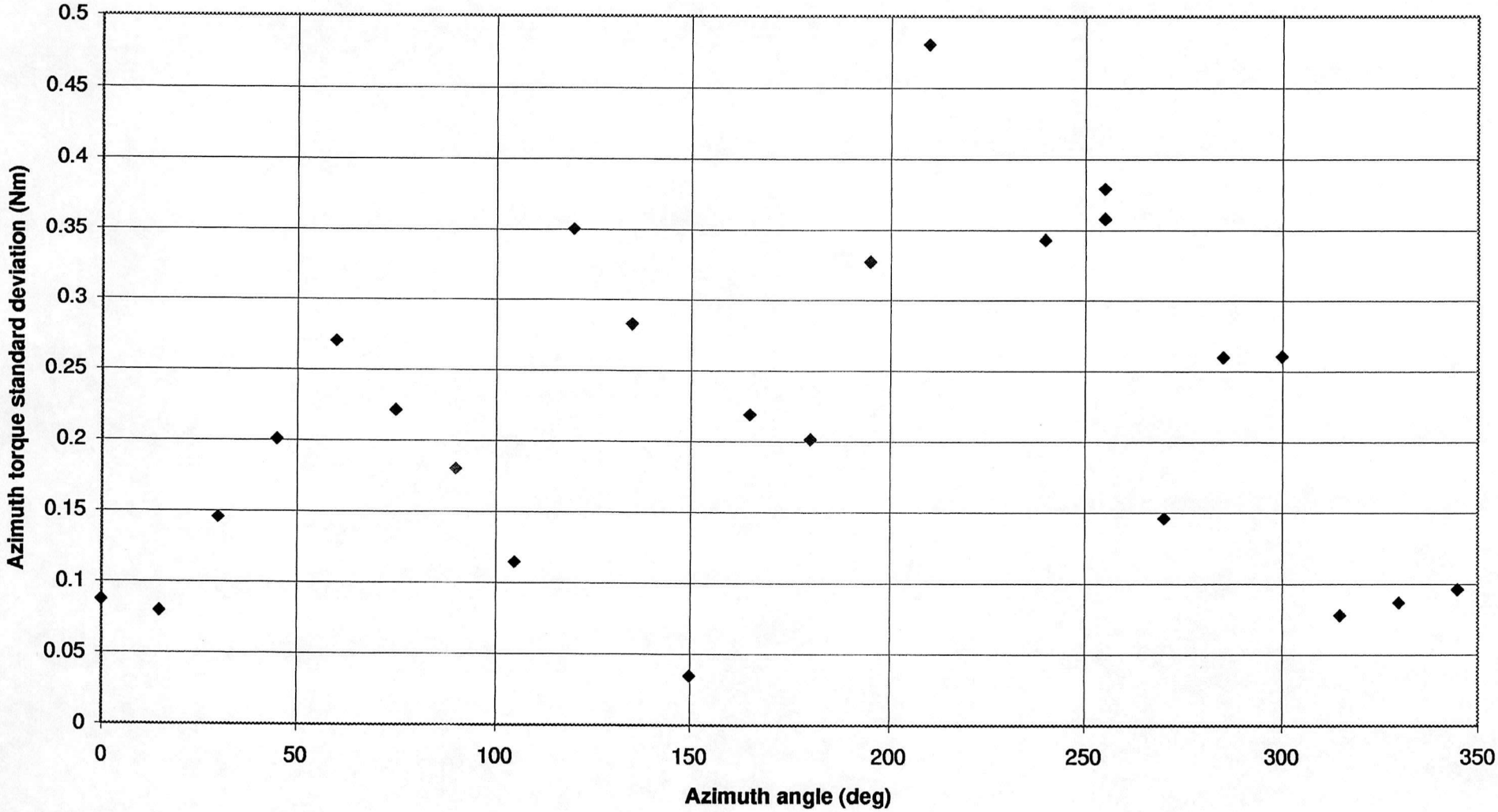

Fig 34. LARGE TURRET: Elevation torque standard deviation at elevation angle of -45 degrees

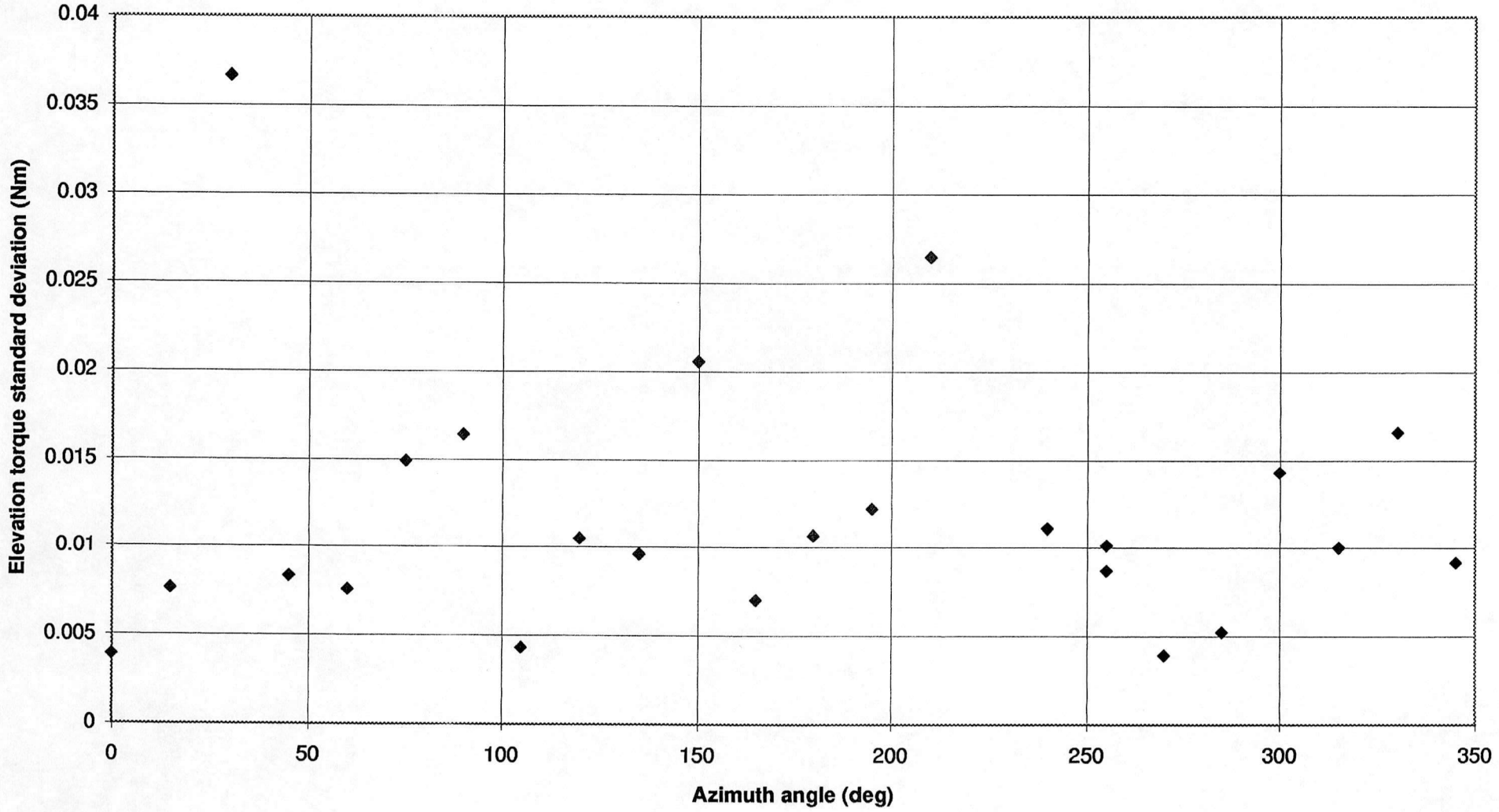

Fig 35. LARGE TURRET: Azimuth torque standard deviation at elevation angle of -90 degrees

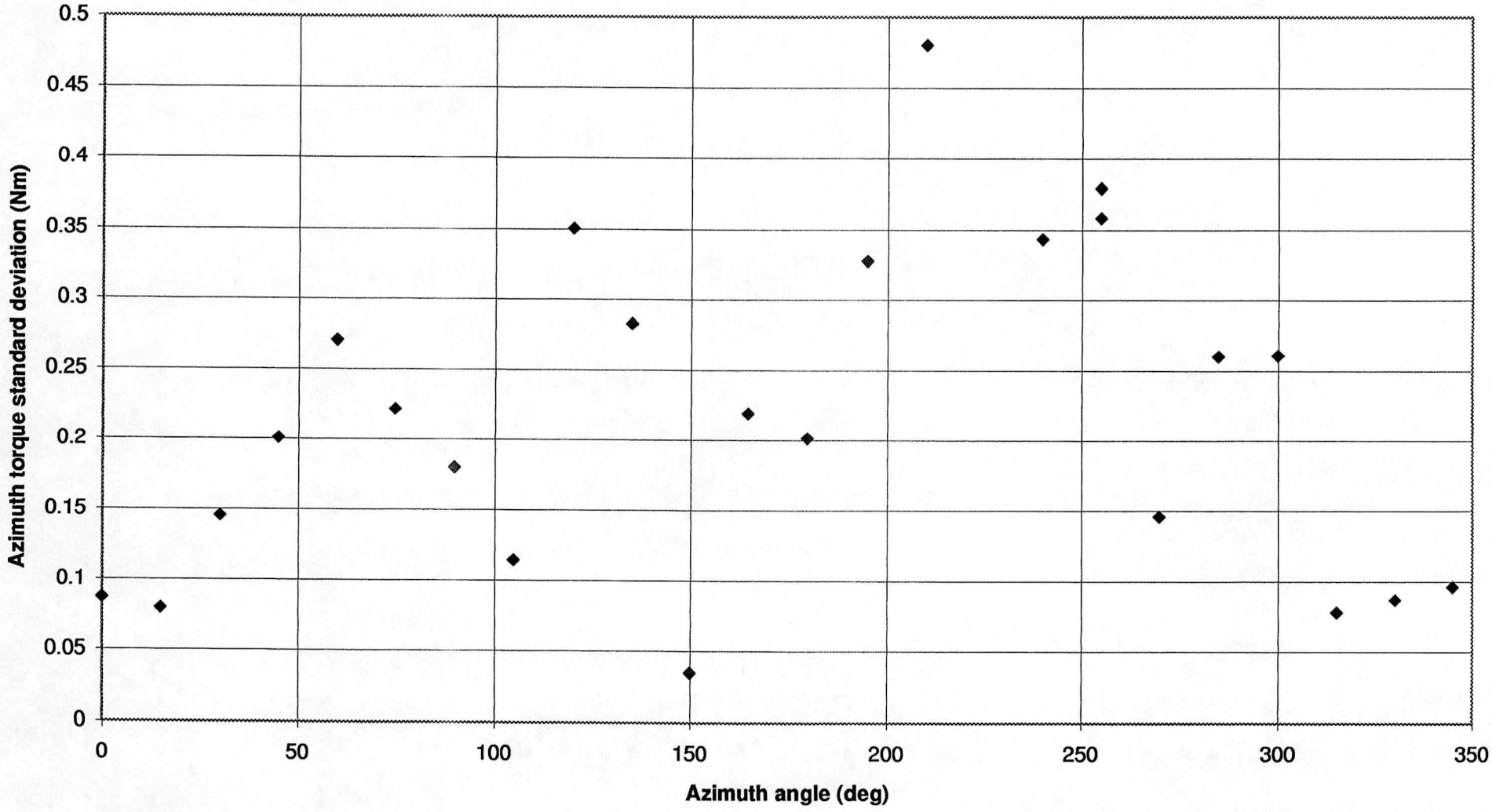

Fig 36. LARGE TURRET: Elevation torque standard deviation at elevation angle of -90 degrees

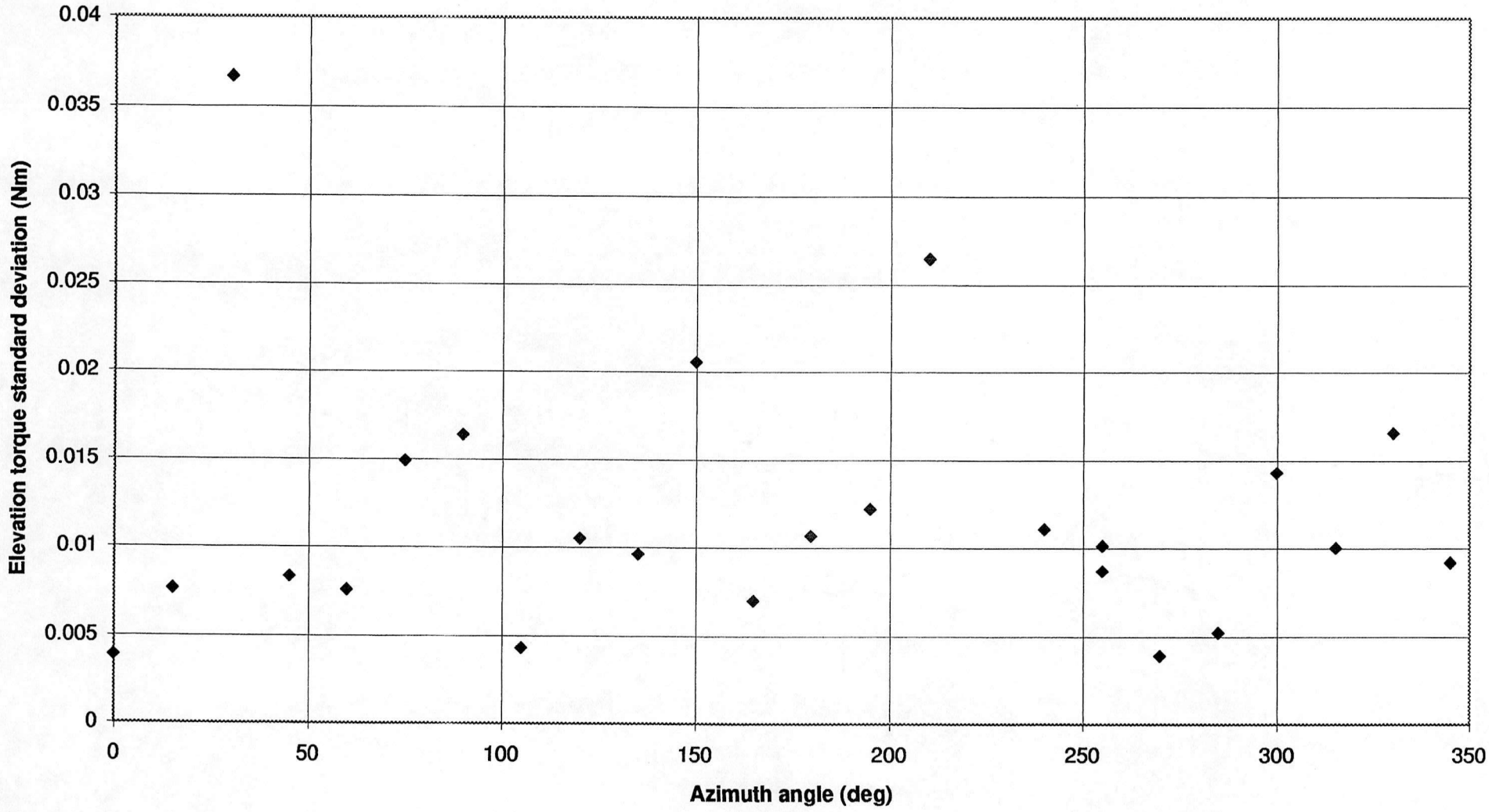

Fig 37. LARGE TURRET: Azimuth torque standard deviation at elevation angle of 45 degrees

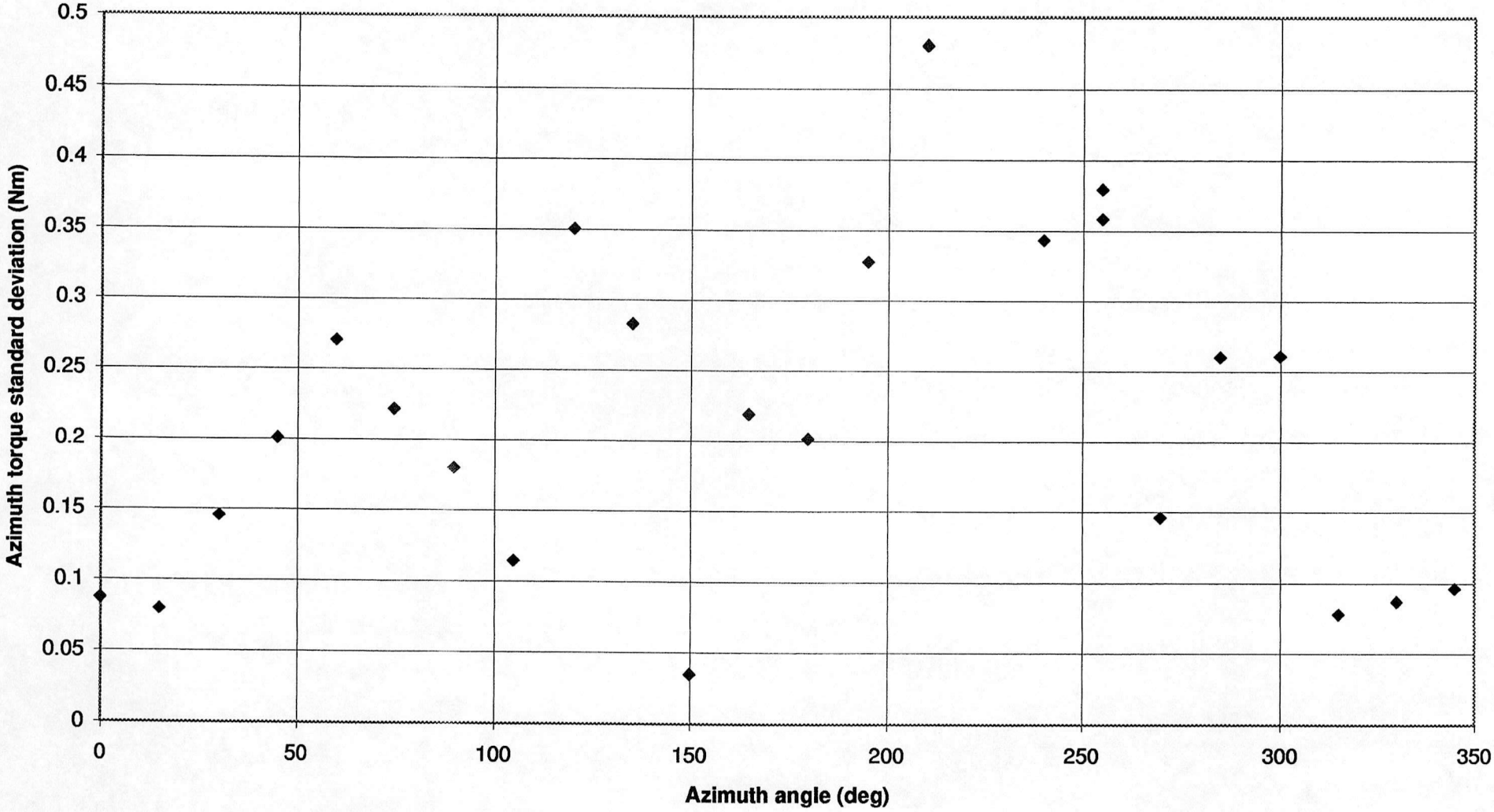

Fig 38. LARGE TURRET: Elevation torque standard deviation at elevation angle of 45 degrees

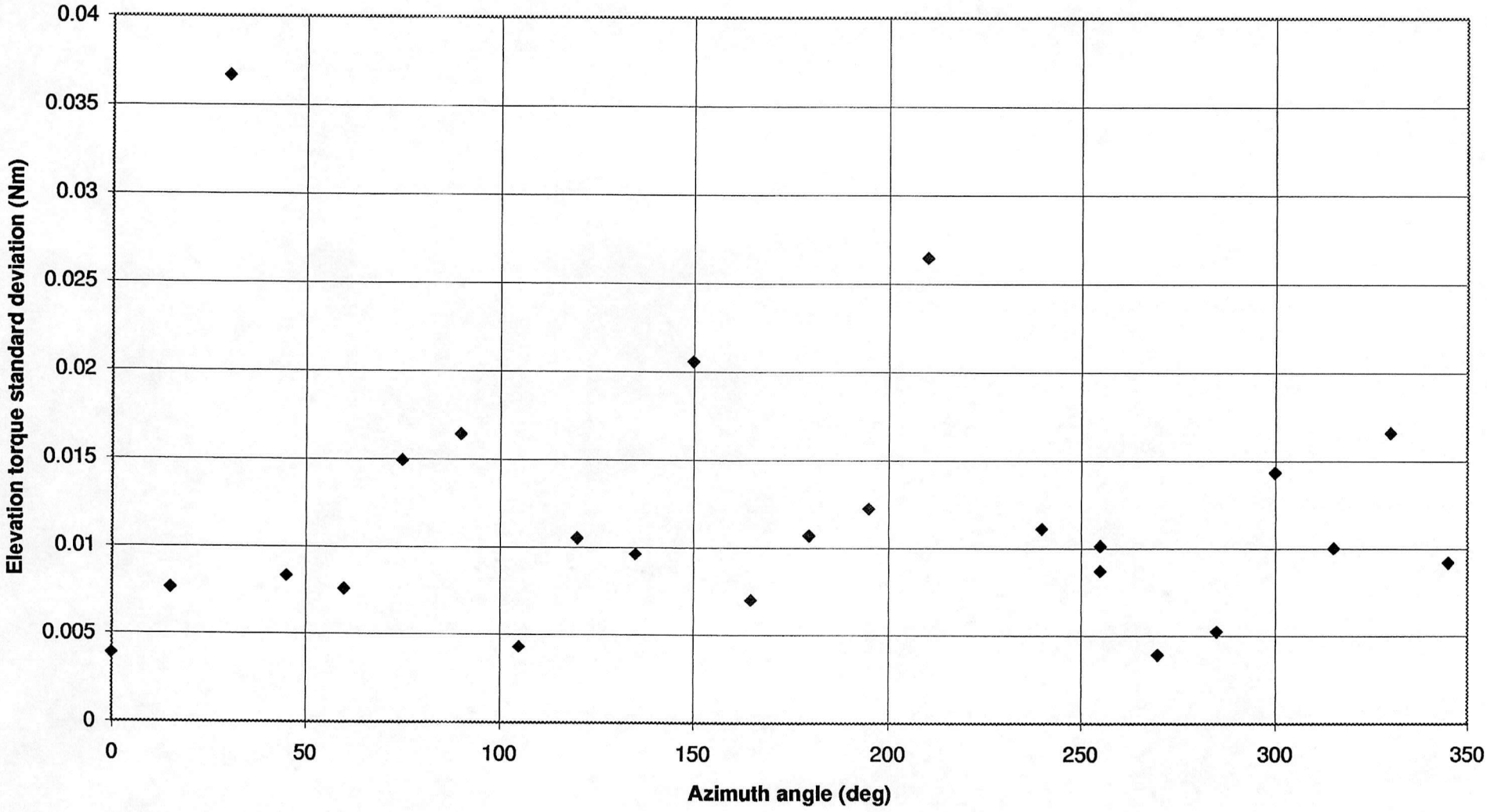

Fig 39. LARGE TURRET: Azimuth torque standard deviation at elevation angle of 90 degrees

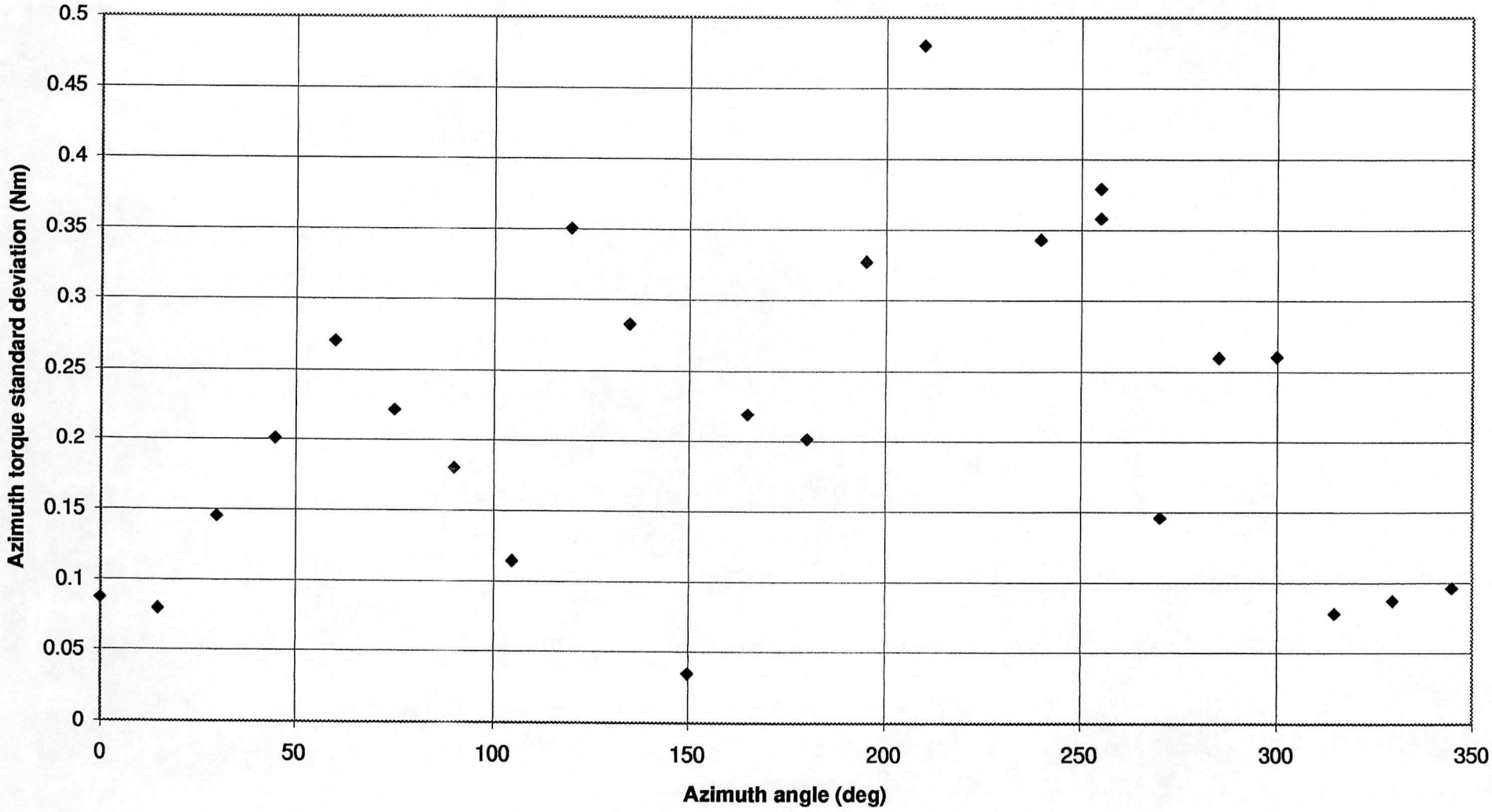

Fig 40. LARGE TURRET: Elevation torque standard deviation at elevation angle of 90 degrees

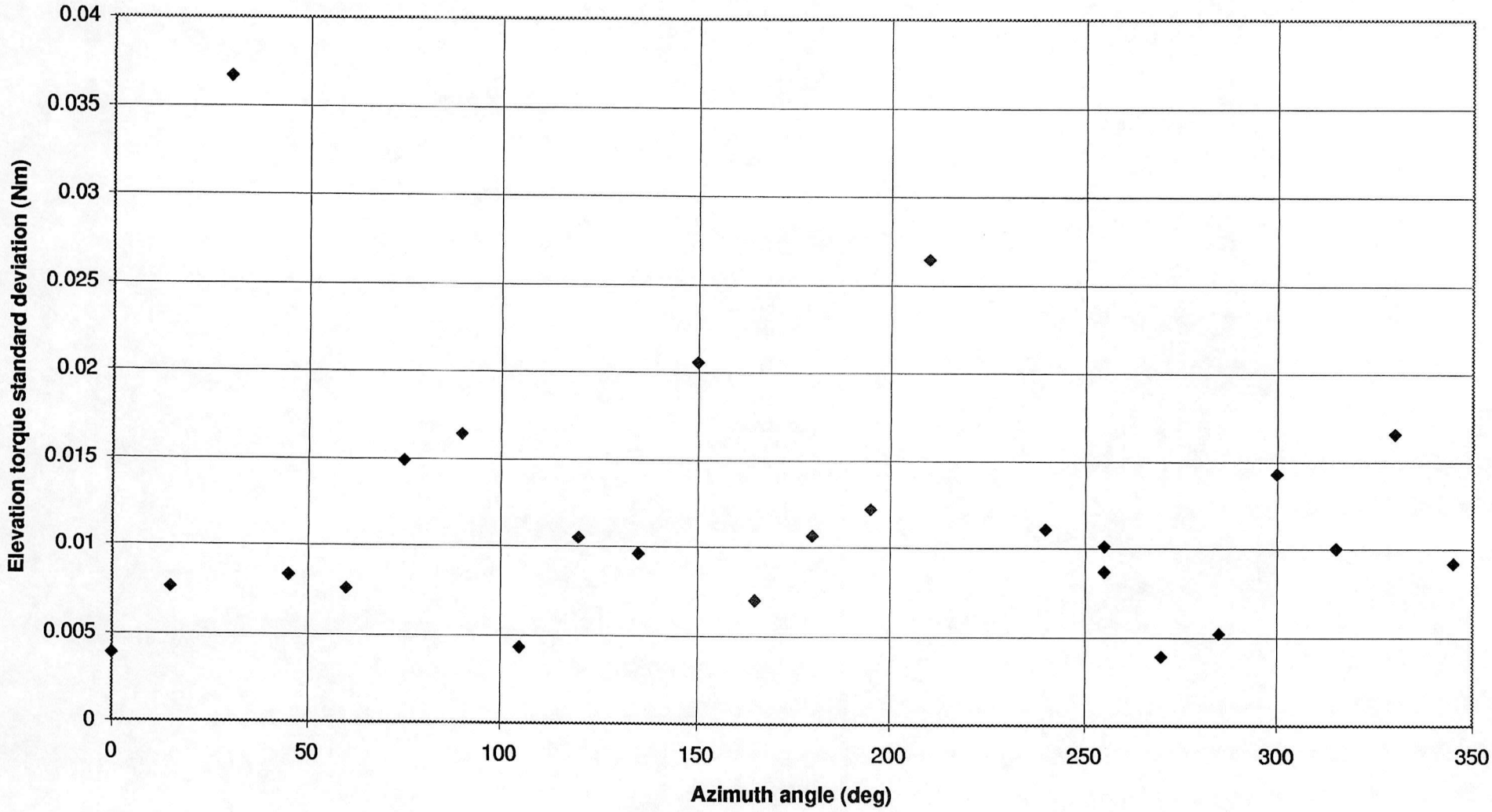

fig 41. SMALL TURRET: Combined azimuth torque data

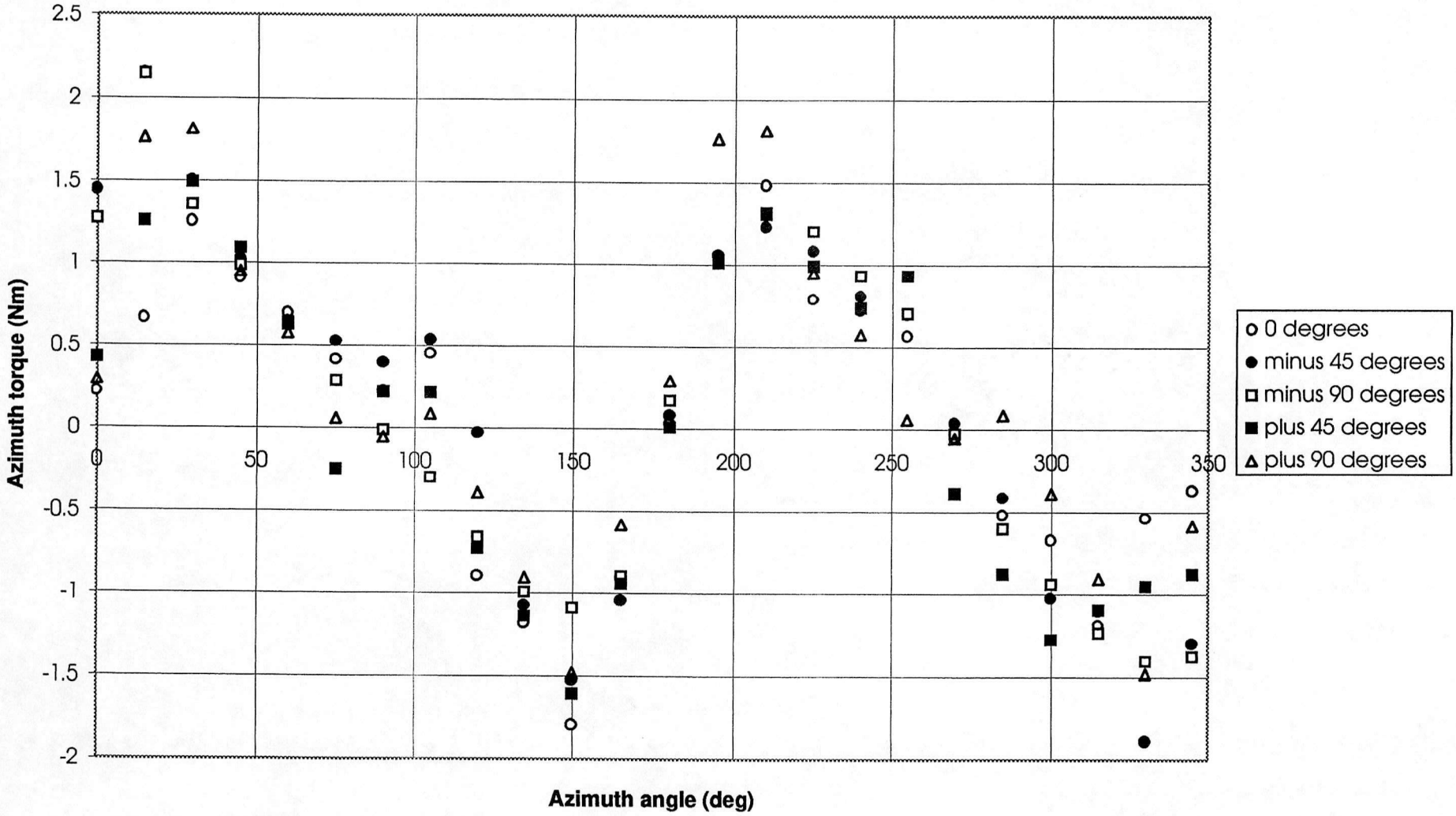

fig 42. SMALL TURRET: Combined elevation torque data

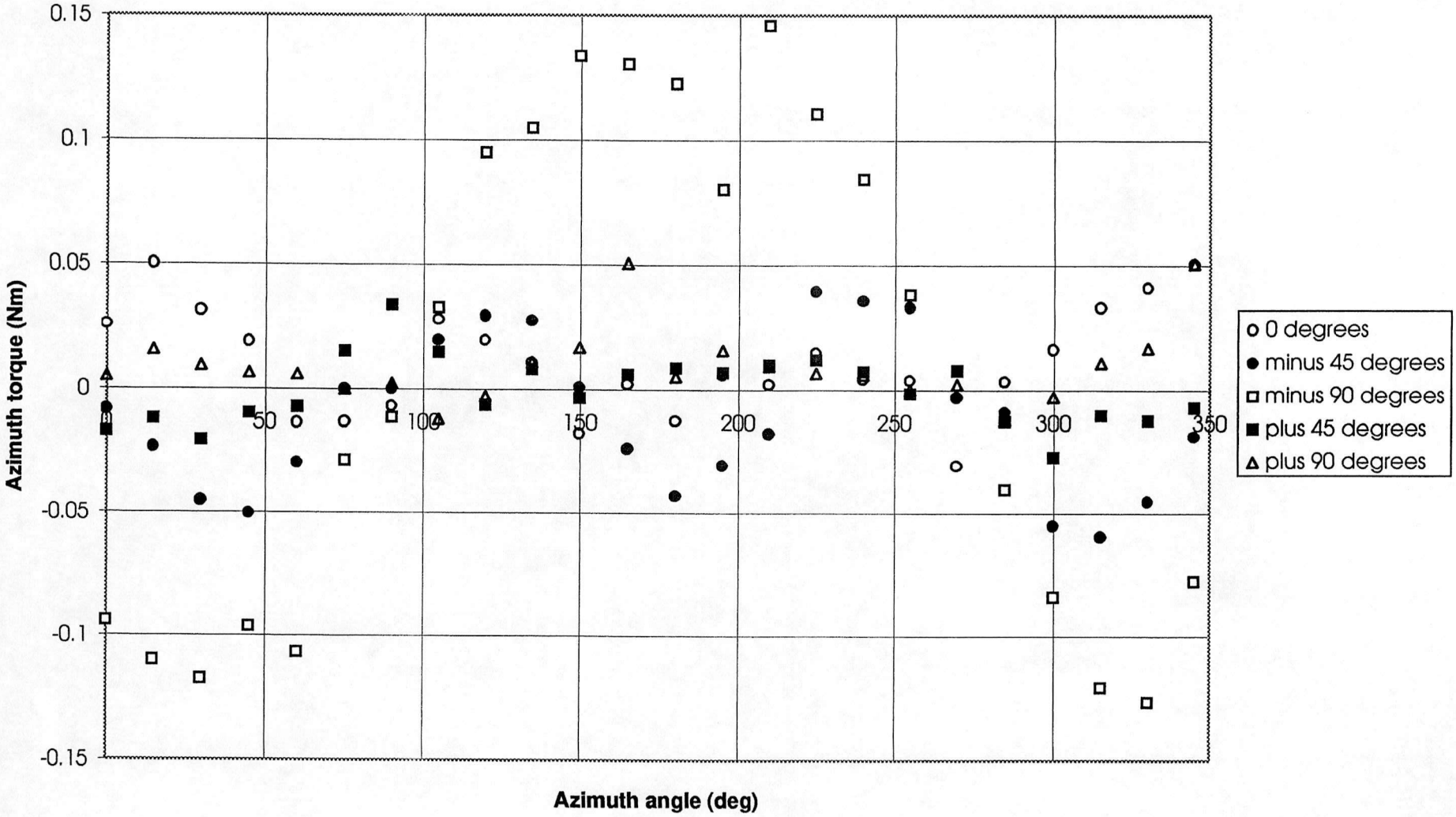

fig 43. SMALL TURRET: Combined Azimuth torque standard deviation data

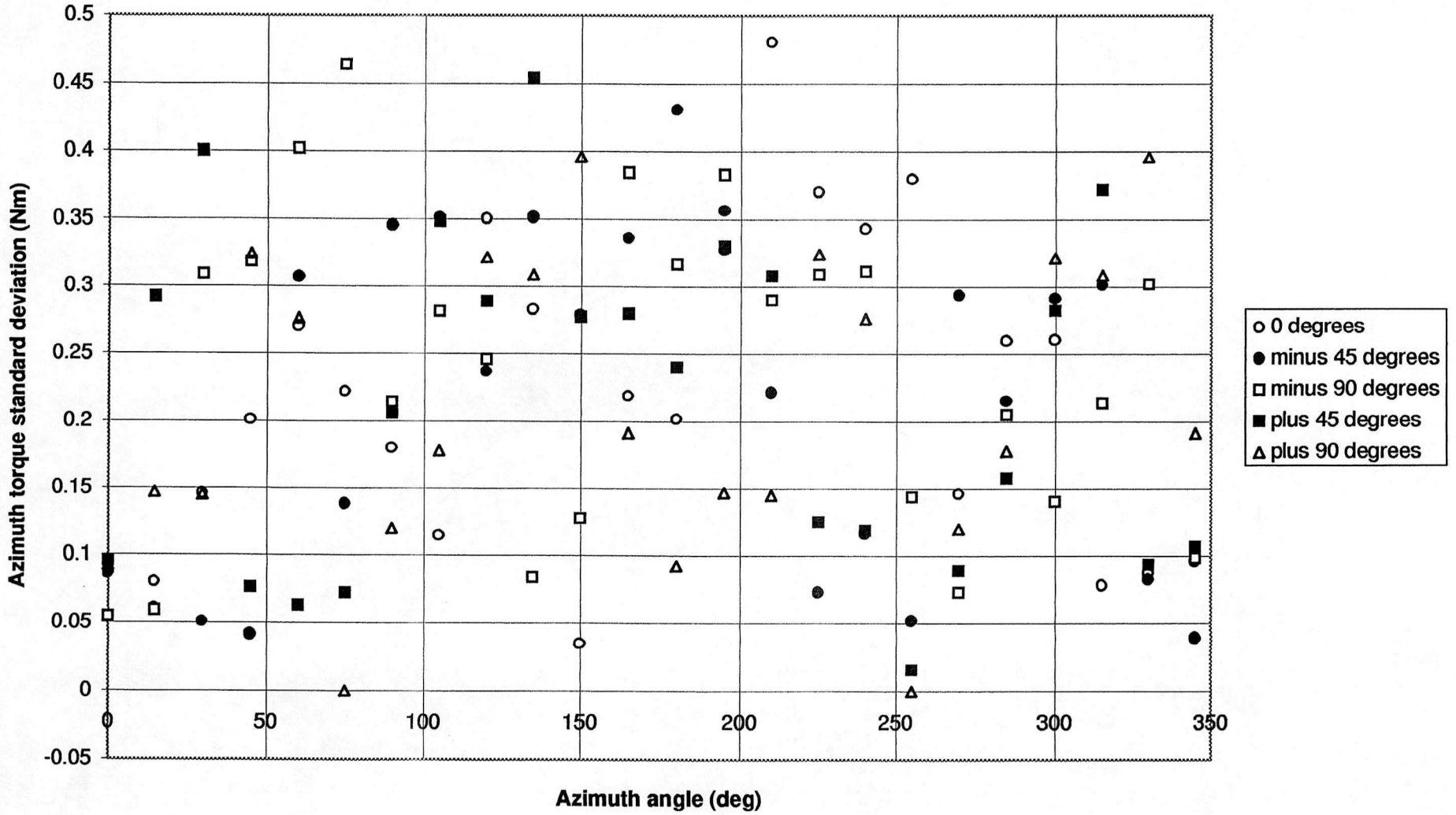

fig 44. SMALL TURRET: Combined elevation torque standard deviation data

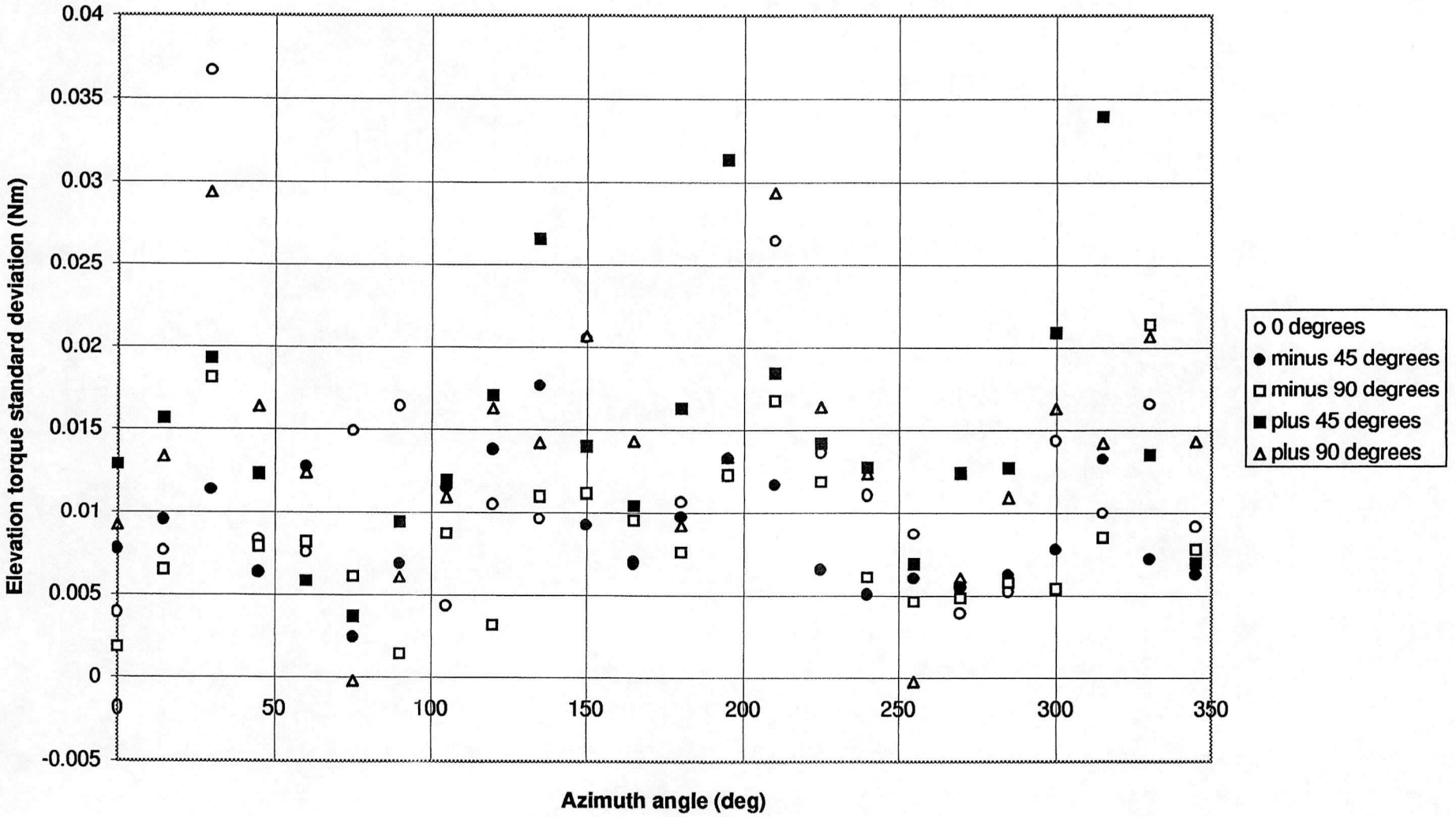

fig 45. LARGE TURRET: Combined azimuth torque data

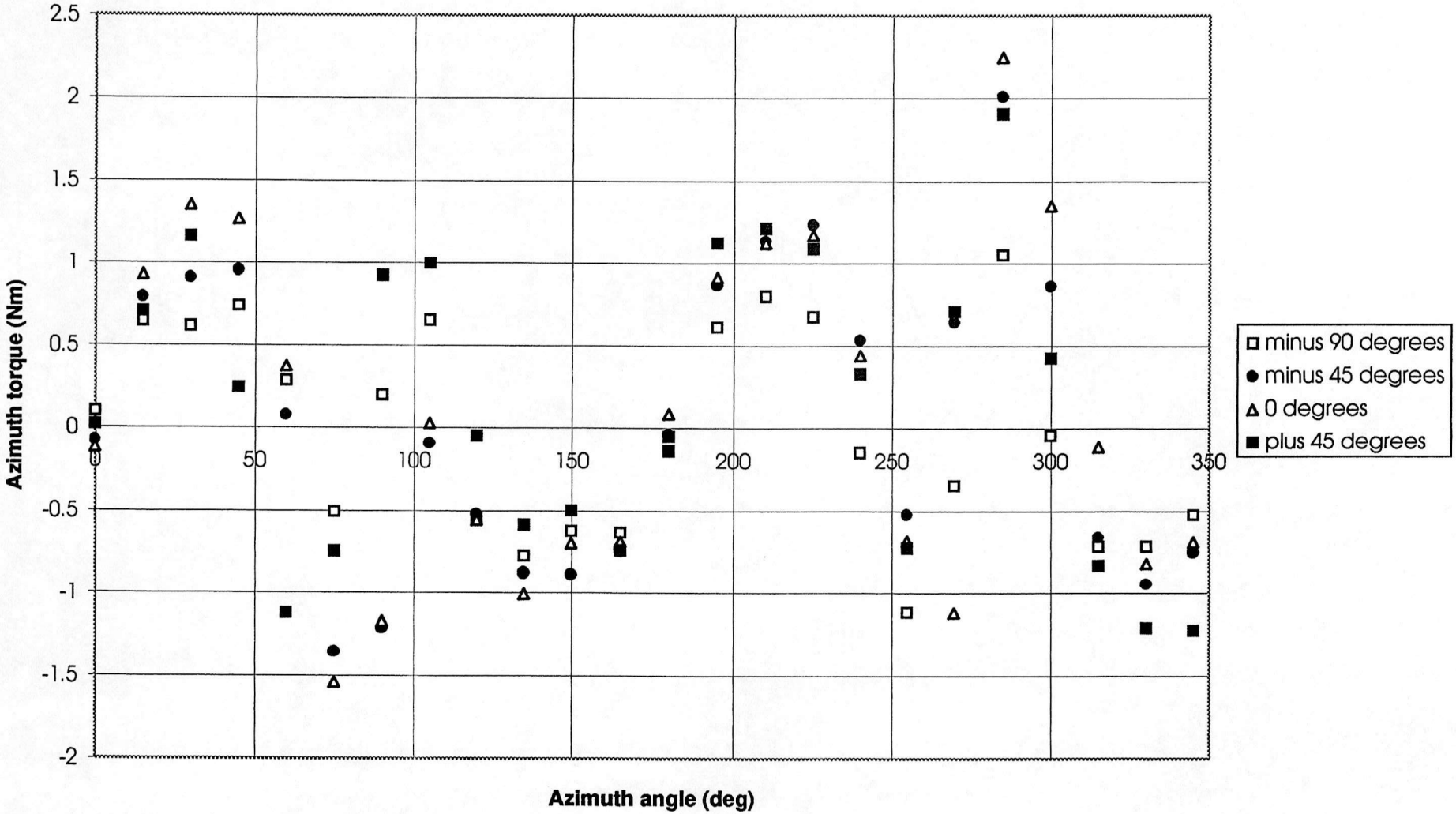

fig 46. LARGE TURRET: Combined elevation torque data

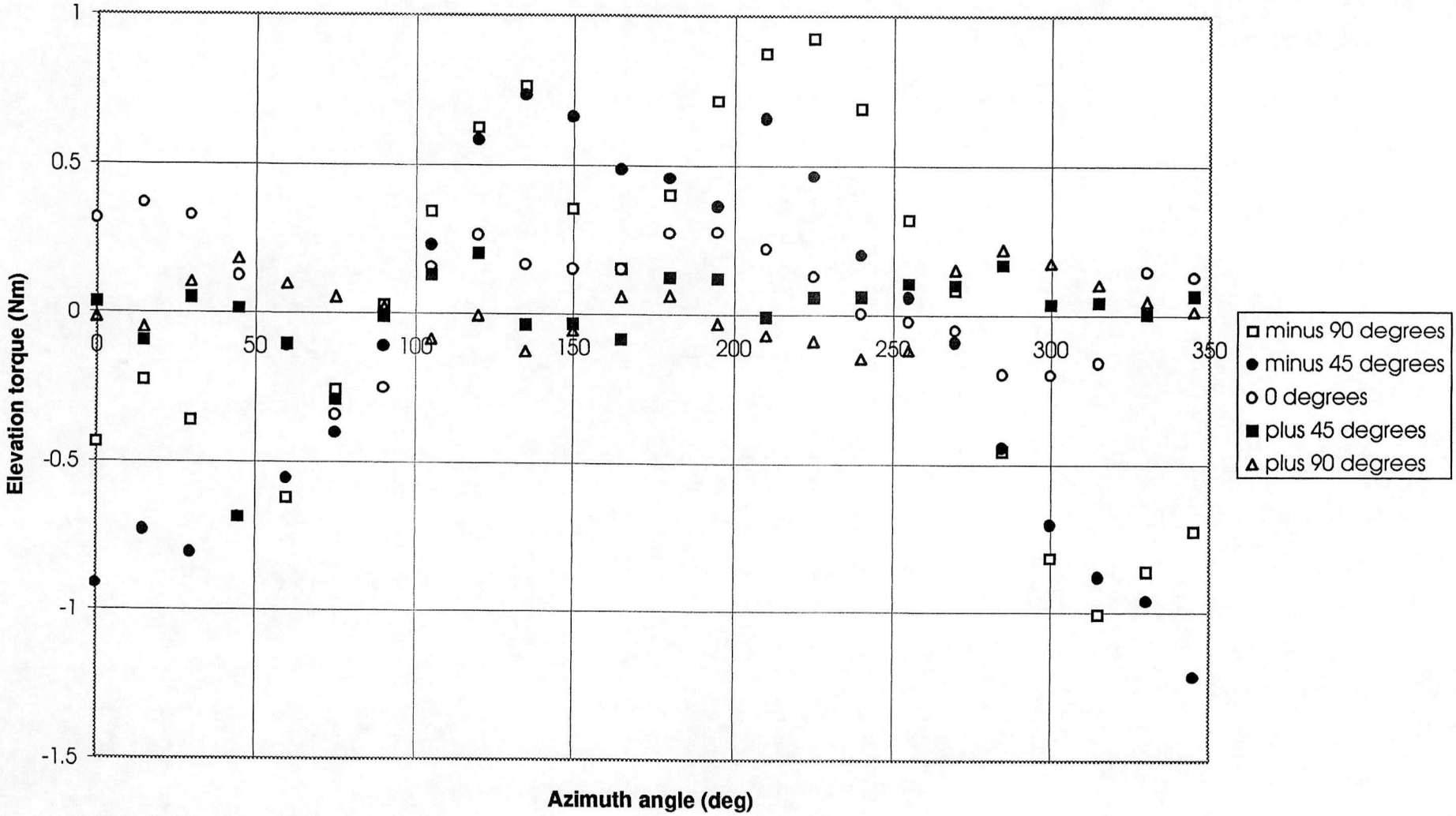

fig 47. LARGE TURRET: Combined azimuth torque standard deviation data

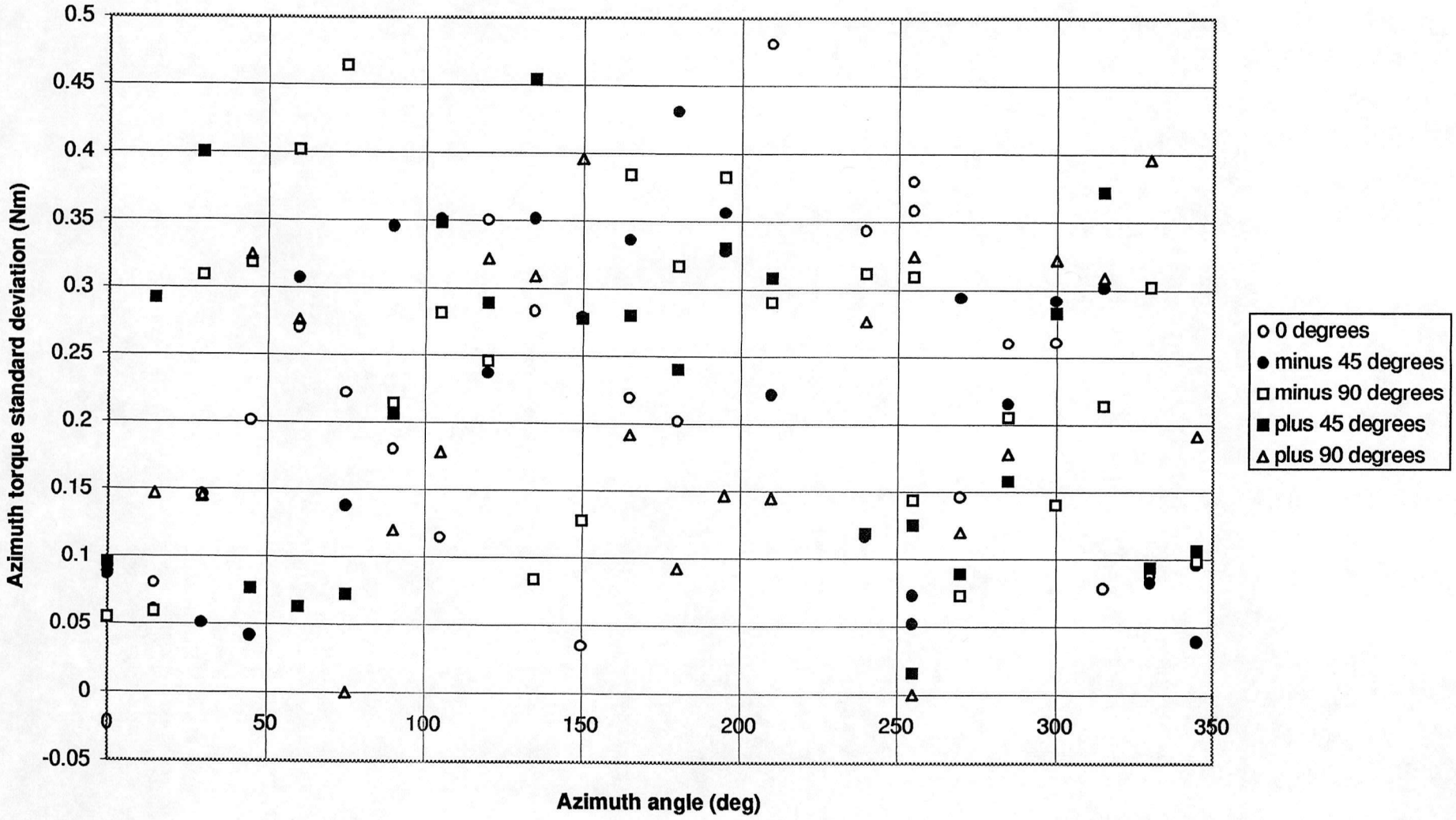

fig 48. LARGE TURRET: Combined elevation torque standard deviation data